

guinea pig, 1:100; Progen), anti-ubiquitin 2 (UBQLN-2 5F5, monoclonal mouse, 1:5000; Abnova), and anti-choline acetyltransferase (ChAT, polyclonal goat, 1:100; Millipore). Diaminobenzidine (Wako) was used as the chromogen.

Antigens were retrieved with trypsin for anti-CD68 immunohistochemistry and with 95°C 3 mmol/L citrate buffer at 95°C for 20 minutes, followed by 5-minute incubation in 98% formic acid for anti-p62N, anti-TDP-43, anti-pTDP-43, and anti-ChAT immunohistochemistry. To confirm the presence of TDP-43-positive inclusions within the cholinergic motor neurons, we performed double immunohistochemistry using anti-pTDP-43 and anti-ChAT antibodies. Spinal cord specimens were prepared from 3 patients with type A, 3 with type B, and 2 with type C. Initially, the specimens were immunostained with the anti-ChAT and anti-goat immunoglobulin antibodies and diaminobenzidine. The anti-ChAT antibody was inactivated in distilled water at 100°C for 20 minutes, followed by immunohistochemistry with pTDP-43 and violet pigmentation using a VIP Peroxidase Substrate Kit (SK-4600; Vector).

For the semiquantitative neuropathological analysis, 2 investigators (Y.R. and M.Y.) observed the specimens containing the facial and hypoglossal nuclei and the anterior horn of the spinal cord. They evaluated the severity of LMN neuropathological changes that are indicative of ALS (neuronal loss, gliosis, aggregation of macrophages, TDP-43-immunopositive neuronal inclusions, and Bunina bodies) and graded neuronal loss and gliosis using Klüver-Barrera and hematoxylin-eosin staining. The investigators also evaluated the aggregations of macrophages rather than rod-shaped microglia using anti-CD68 immunohistochemistry and identified Bunina bodies using hematoxylin-eosin staining and anti-cystatin C immunohistochemistry. They scored the severity of neuronal loss and gliosis as grade 0 (none), 1 (mild), 2 (moderate), or 3 (severe) (eFigure 1 in Supplement). The appearance of TDP-43-positive inclusions was scored as grade 0 (none), grade 1 (1-5 neuronal inclusions per 5 fields;  $\times 20$  objective), grade 2 (6-10 inclusions), or grade 3 ( $\geq 11$  inclusions) using anti-pTDP-43 immunohistochemistry.

Pathological cortical TDP-43 subtypes were identified according to current neuropathological criteria, using specimens from the frontal lobes, temporal lobes, and hippocampus.<sup>5</sup> For FTLD-TDP, type A was defined as the presence of neuronal cytoplasmic inclusions predominantly in the neocortex layer 2 and short dystrophic neurites; type B, as a predominance of neuronal cytoplasmic inclusions in all cortical layers; and type C, as a predominance of long dystrophic neurites in layer 2 and cytoplasmic inclusions in the dentate granular cells of the hippocampus. Our patient series did not include type D, which is characterized by numerous short dystrophic neurites and neuronal intranuclear inclusions in association with valosin-containing protein gene mutations. We also evaluated pathological changes in the upper motor neuron systems that include the primary motor cortex and corticospinal tract (CST). We evaluated the presence or absence of neuronal loss and gliosis in the primary motor cortex and myelin pallor, as well as the aggregation of macrophages in the CST.

### Immunohistochemical Screening of Hexanucleotide Repeat Expansion Sequence in Chromosome 9 Open Reading Frame 72

Our study focused on sporadic FTLD-TDP, and patients with familial histories of FTLD or ALS, dementia, or other neurodegenerative diseases were excluded. However, FTLD or ALS associated with chromosome 9 open reading frame 72 (C9ORF72) hexanucleotide expansion exhibits pathological aggregation of TDP-43 and, in some cases, low penetration,<sup>20,21</sup> although these mutations are extremely rare in Japan.<sup>22</sup> It was recently reported that the pattern of ubiquitin abnormalities in ALS and FTLD corresponds well with the presence of C9ORF72 hexanucleotide expansion.<sup>23</sup> The UBQLN-2-positive, p62-positive, but TDP-43-negative thick dystrophic neurites are abundantly present in patients with C9ORF72 hexanucleotide expansion, predominantly in the hippocampus and cerebellum. Because the materials for a genetic study were not available for a large proportion of our patients, we histologically screened C9ORF72 hexanucleotide expansion with the absence of UBQLN-2 and p62N-positive thick dystrophic neurites in the temporal lobes and cerebella of all patients.

### Statistical Analysis

The Mann-Whitney test was applied to continuous variables between 2 groups, and the Kruskal-Wallis test was applied to the analysis of continuous variables among 3 groups. The  $\chi^2$  test was used for categorized variables among 3 groups. Spearman rank correlation coefficient analyses were applied to univariate correlations between the clinical groups and severity of pathological changes. Survival curves were constructed using the Kaplan-Meier method. The end point of clinical course was defined as death or the introduction of a respirator or tracheotomy. The significance level for all comparisons was set at  $P < .05$ . All statistical tests were 2 sided and were conducted using the PASW 18.0 program (IBM SPSS).

## Results

### Clinical Analysis

Patient characteristics are summarized in the **Table**. The mean (SD) time from symptom onset to death or respirator or tracheotomy administration was 50.5 (58.4) months across all patients. The survival time from symptom onset did not differ significantly between the FTLD-ALS and ALS-FTLD groups but was significantly shorter for the FTLD without ALS group than for the FTLD-ALS or ALS-FTLD group (**Figure 1** and **Table**;  $P < .001$ ). The most common cause of death for the ALS-FTLD and FTLD-ALS groups was respiratory failure, but patients with FTLD without ALS commonly died of other systemic diseases ( $P < .001$ ). Frequencies of dementia subtypes did not significantly differ between the clinical groups.

With regard to motor symptoms/signs, 3 patients in the FTLD without ALS group had hyperreflexia, 1 had the Babinski sign, and 1 had spasticity, but none had a clinical diagnosis of progressive lateral sclerosis (PLS) according to the published diagnostic criteria of PLS.<sup>24</sup> Patients with FTLD-ALS or

Table. Clinical and Demographic Patient Characteristics

Characteristic	Patient Group			P Value
	FTLD Without ALS (n = 11)	FTLD-ALS (n = 9)	ALS-FTLD (n = 23)	
Sex, No. female/male <sup>a</sup>	8/3	3/6	10/13	.16
Age at onset, mean (SD), y <sup>b</sup>	62.4 (9.4)	58.2 (11.3)	61.2 (9.5)	.79
Clinical duration without respirator or tracheotomy, median (range), mo <sup>c</sup>	84.0 (47.0-360.0)	28.0 (7.0-60.0)	22.0 (7.0-71.0)	<.001
Duration between FTLD and ALS, median (range), mo <sup>d</sup>		18.0 (4.0-48.0)	19.0 (0-60.0)	.92
Patients with tracheotomy, No. (%) <sup>a</sup>	0	0	2 (9)	.40
Patients with respirators, No. (%) <sup>a</sup>	0	1 (11)	8 (35)	.047
Duration with respirator or tracheotomy, median (range), mo		30.0	39.0 (1.0-141.0)	...
Causes of death, No. (%) <sup>a</sup>				
Respiratory failure	0	6 (67)	20 (87)	<.001
Pneumonia	3 (27)	3 (33)	3 (13)	.37
Other	8 (73)	0	0	<.001
Subtypes of dementia, No. (%)				
Behavior-variant FTD	7 (64)	7 (78)	19 (83)	.29
Language impairments	4 (36)	2 (22)	4 (17)	.62
Motor symptoms/signs, No. (%)				
Muscle weakness <sup>a</sup>	0	9 (100)	23 (100)	<.001
Muscle atrophy	0	7 (78)	22 (96)	<.001
Fasciculation	0	4 (44)	15 (65)	.002
Hyperreflexia	3 (27)	5 (56)	17 (74)	.009
Babinski sign	1 (9)	4 (44)	3 (13)	.08
Spasticity	1 (9)	0	1 (4)	.63
Electromyography, No. (%)				
Total examined	2 (18)	4 (82)	21 (91)	...
Active denervation <sup>a</sup>	0	3 (75)	12 (57)	.054

Abbreviations: ALS, amyotrophic lateral sclerosis; ALS-FTLD, onset of ALS symptoms/signs preceding those of frontotemporal lobar degeneration (FTLD); ellipses, not significant; FTD, frontotemporal dementia; FTLD-ALS, onset of FTLD symptoms/signs preceding those of ALS.

<sup>a</sup>  $\chi^2$  Test.

<sup>b</sup> Kruskal-Wallis test.

<sup>c</sup> Log-rank test.

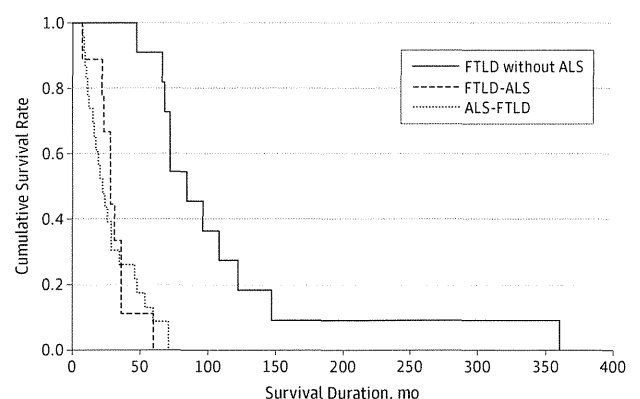
<sup>d</sup> Mann-Whitney test.

ALS-FTLD generally exhibited both upper motor neuron and LMN symptoms/signs except for 3 who exhibited only LMN symptoms/signs. Based on the electromyographic data, active denervation potentials (positive sharp waves and fibrillation potentials<sup>18</sup>) were identified in 3 patients with FTLD-ALS and 12 with ALS-FTLD but not in any of those with FTLD without ALS.

#### Pathological Evaluations of the LMN System

The results of semiquantitative pathological evaluations of the 3 clinical groups are summarized in **Figure 2**. In the FTLD without ALS group, 8 of 9 patients (89%) showed pTDP-43-positive neuronal inclusions. In addition, neuronal loss and gliosis in the spinal anterior horns were observed in 5 of 11 patients (45%) and Bunina bodies were present in 4 (36%). The pathological changes in LMN systems were most severe in the ALS-FTLD group, followed by the FTLD-ALS group, and were rather mild in the FTLD without ALS group. Among control patients, 1 had a pTDP-43-positive glial inclusion in the lumbar anterior horn, but this patient did not show neuronal loss, gliosis, or Bunina bodies (eFigure 2 in Supplement).

Figure 1. Survival by Clinical Group



Kaplan-Meier plot showing the survival rates of patients with frontotemporal lobar degeneration (FTLD) without amyotrophic lateral sclerosis (ALS) (solid line; n = 11), those in whom the onset of FTLD symptoms/signs preceded those of ALS (FTLD-ALS) (dashed line; n = 9), and those in whom the onset of ALS symptoms/signs preceded those of FTLD (ALS-FTLD) (dotted line; n = 23). Survival times were significantly shorter in patients with FTLD without ALS than in those with FTLD-ALS or ALS-FTLD ( $P < .001$ ).

Figure 2. Semiquantitative Evaluations of Pathological Changes by Clinical Group

Patients	FTLD Without ALS									FTLD-ALS						ALS-FTLD						P Values	r Values									
	1	2	3	4	5	6	7	8	9	10	11	12	13	14	15	16	17	18	19	20	21			22	23	24	25	26	27	28	29	
Clinical duration, mo	47	66	84	108	147	360	68	96	122	22	23	28	28	31	36	36	60	7	8	9	10	16	20	22	24	26	54	60	71			
Neuronal loss																																
Facial nuclei	+	-	-	-	+	-	-	-	-	++	NA	+	+	+	+	++	+	+	++	+	+	++	++	NA	++	+	+++	+++	+	<.01	0.730	
Hypoglossal nuclei	-	-	-	-	-	-	-	-	-	+++	NA	++	+++	+++	+	+++	++	+++	+	+	+++	+++	+++	+++	++	+++	+++	+++	++	<.01	0.823	
Anterior horn of Cx	+	++	-	-	+	-	-	-	+	++	++	+	++	++	+	++	+	+++	++	++	++	++	++	NA	+++	+++	++	+++	++	<.01	0.804	
Anterior horn of Tx	+	+	NA	+	+	-	NA	-	+	+	++	++	++	++	++	+	++	++	+	+++	++	++	++	++	++	+++	+++	+++	++	<.01	0.768	
Anterior horn of Lx	-	-	NA	+	+	-	NA	-	-	+	+	+	+	+	+	++	+	++	++	++	+	++	++	NA	++	+++	+++	++	++	<.01	0.856	
Anterior horn of Sx	-	-	NA	+	-	-	NA	-	-	+	NA	+	+	+	+	++	+	++	++	NA	NA	++	++	NA	++	++	+++	NA	+	<.01	0.880	
Gliosis																																
Facial nuclei	++	-	-	-	+	-	-	-	-	++	NA	+	+	+	+	++	+	++	++	+	++	++	++	NA	+	++	+++	+++	++	<.01	0.768	
Hypoglossal nuclei	-	-	-	-	-	-	-	-	-	+++	NA	++	+++	+++	+	+++	++	+++	+	+	+++	+++	+++	+++	++	+++	+++	+++	++	<.01	0.828	
Anterior horn of Cx	+	++	-	-	+	-	-	-	+	++	++	+	+++	++	+	++	+	+++	+	++	++	++	++	NA	++	+++	+++	+++	++	<.01	0.730	
Anterior horn of Tx	+	+	NA	-	+	-	NA	-	+	+	++	++	++	++	++	+	++	++	+	+++	++	++	++	++	+	+++	+++	+++	++	<.01	0.740	
Anterior horn of Lx	-	-	NA	+	+	-	NA	-	-	+	+	+	+	+	+	++	+	++	++	++	++	++	++	++	++	+++	+++	+++	++	<.01	0.878	
Anterior horn of Sx	-	-	NA	+	-	-	NA	-	-	+	NA	+	+	+	+	++	+	++	++	NA	NA	++	++	NA	++	+++	+++	+++	NA	++	<.01	0.904
pTDP-43-positive neuronal inclusions																																
Facial nuclei	+	-	-	-	+	-	-	-	-	++	NA	+	+	+	+	+	+	+	++	+	++	+++	+	NA	+	++	+	+	++	<.01	0.729	
Hypoglossal nuclei	-	+	+	-	-	-	+	-	-	+	NA	+	+	+	++	+	+	+	-	+	+++	+	-	+	+	-	+	+	.08	0.348		
Anterior horn of Cx	+	+	+	+	+	-	+	+	-	++	++	++	++	++	++	++	++	++	+++	+	+++	++	++	NA	+	+	+	+	+	<.01	0.511	
Anterior horn of Tx	+	+	NA	-	+	-	NA	+	+	+	+	++	+	+	+	+	+	+	+	+	++	+	++	+	+	+	+	+	+	<.05	0.403	
Anterior horn of Lx	+	+	NA	+	-	-	NA	+	+	+	+	+++	+++	+++	+	+++	+	+	+++	+++	+++	+++	+++	NA	+	+	+	+++	+	<.05	0.412	
Anterior horn of Sx	+	-	NA	-	-	-	NA	+	-	++	NA	++	+	+	+	+	+	+	+	NA	NA	+	+++	NA	-	+	+	NA	+	<.05	0.458	
Aggregation of macrophages																																
Facial nuclei	++	-	+	-	+	-	-	-	-	++	NA	+	-	++	+	+++	+	++	+	+	+	++	NA	+	++	++	+	+	+	<.01	0.518	
Hypoglossal nuclei	+	-	-	-	-	-	-	-	-	+	NA	-	+	++	+	+	-	+++	+	++	+	+	+++	-	++	+++	++	+	-	<.01	0.634	
Anterior horn of Cx	+	+	-	+	+	-	+	+	+	++	+	+	++	++	++	++	++	+	+	+	+	-	++	NA	+	+	+	-	-	0.78	0.073	
Anterior horn of Tx	+	+	NA	-	-	-	NA	+	+	++	++	++	++	++	++	++	++	+	+	++	++	+	++	+	+	+	+	+	+	<.05	0.435	
Anterior horn of Lx	-	++	NA	+	-	-	NA	-	-	+	-	-	+	+	++	+	+	+++	++	+++	++	+	+++	+	+	+++	+++	+++	++	<.01	0.721	
Anterior horn of Sx	-	+	NA	+	-	-	NA	-	-	+	NA	-	+	+	+	+	+	+++	++	NA	NA	+	++	NA	+	+++	+++	+++	NA	+	<.01	0.751
Bunina bodies	+	+	-	+	+	-	-	-	-	+	+	+	+	-	+	+	+	+	+	+	+	+	+	-	+	+	+	+	+			
Brain TDP-43 disease type	A	A	A	A	A	A	C	C	C	B	B	B	B	B	B	B	B	B	B	B	B	B	B	B	B	B	B	B	B	B		

Findings shown include the severity of neuronal loss, gliosis, phosphorylated TAR DNA-binding protein of 43 kDa (pTDP-43) pathological changes, and aggregations of macrophages and the presence of Bunina bodies in the lower motor neuron systems. The severity of each pathological change was graded as 0 (none [-, not colored]), 1 (mild [+ , green]), 2 (moderate [++ , yellow]), or 3 (severe [+++ , red]). Neuropathological changes became increasingly severe in

those in whom amyotrophic lateral sclerosis (ALS) symptoms/signs preceded those of frontotemporal lobar degeneration (FTLD; ALS-FTLD), as well as the FTLD-ALS (FTLD symptoms/signs preceding those of ALS) and FTLD without ALS groups (Spearman rank order). Cx indicates cervical cord; Lx, lumbar cord; NA, not assessed; Sx, sacral cord; TDP-43, TAR DNA-binding protein of 43 kDa; and Tx, thoracic cord.

According to cortical TDP-43 pathological findings,<sup>5</sup> 29 patients were classified into 3 subtypes: A (n = 6), B (n = 20), or C (n = 3). Patients with FTLD without ALS showed type A or C disease, whereas those with FTLD-ALS or ALS-FTLD all showed type B disease (Figure 2 and Figure 3). For all the subtypes, the LMN system showed neuropathological changes that were indicative of ALS, including pTDP-43-positive neuronal and glial inclusions, neuronal loss, and gliosis. In patients with type A disease (Figure 4A-H), the severity of neuronal loss and gliosis in LMN systems ranged from none to moderate. Five patients (83%) in this group had pTDP-43-positive, skeinlike cytoplasmic and/or nuclear inclusions (Figure 4B and C), and 4 (67%) had Bunina bodies (Figure 4E and F) in the LMNs.

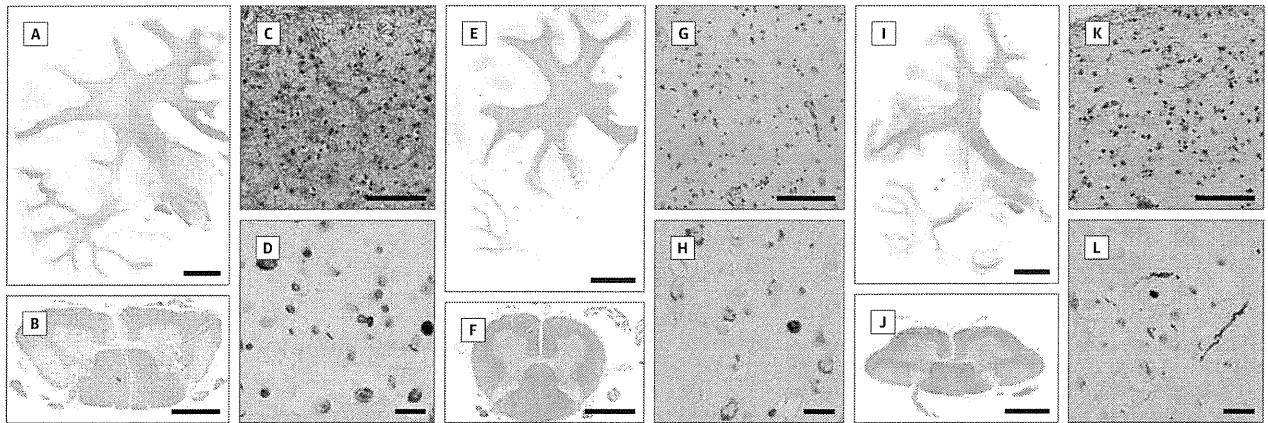
All 20 patients in the type B group (Figure 4I-L) showed neuronal loss, gliosis, and pTDP-43-positive skeinlike cytoplasmic inclusions in the LMN systems, and 18 (90%) had Bunina bodies. Among the 3 patients with type C disease (Figure 4M-P), 1 (33%) had mild loss of the LMNs (Figure 4M), and all 3 (100%) had pTDP-43-positive skeinlike cytoplasmic inclusions in the LMNs (Figure 4N). Unlike patients with the

other subtypes, those with type C disease lacked Bunina bodies. Moreover, thick dystrophic neurites were prominent in the spinal anterior horn in patients with type A or C disease but rarely present in those with type B disease (Figure 4G and O). These dystrophic neurites were larger in diameter (8-12 μm) than those found in the cortices. In a double immunohistochemical analysis, pTDP-43-positive inclusions were found within the cytoplasm of ChAT-positive neurons in patients with type A, B, and C disease (Figure 4H, L, and P).

### Pathological Evaluations of the Upper Motor Neuron System

In the primary motor cortex, neuronal loss and gliosis were evident in 5 patients with FTLD without ALS (56%), 2 with FTLD-ALS (25%), and 3 with ALS-FTLD (25%). Myelin pallor in the CST was evident in 6 patients with FTLD without ALS (67%), 1 with FTLD-ALS (12%), and 2 with ALS-FTLD (17%). Aggregations of macrophages in the CST were evident in 4 patients with FTLD without ALS (44%), 5 with FTLD-ALS (62%), and 6 with ALS-FTLD (50%).

Figure 3. Semimacroscopic Appearances and Brain Pathological Findings in Patients With Type A, B, and C Pathological Changes



Findings in patients with type A (A-D), B (E-H), and C (I-L) pathological changes. In a patient with type A pathological change, cerebral coronal sections showed cortical atrophy of the parasylvian region (A). Transverse section of the cervical cord showed marked myelin pallor in the corticospinal tract (B). Microscopically, the frontal cortices showed marked neuronal loss (C) and phosphorylated TAR DNA-binding protein of 43 kDa (pTDP-43)-positive neuronal inclusions and short dystrophic neurites (D). In a patient with type B pathological change, the cerebral cortex showed severe temporal atrophy (E), neuronal loss (G), and pTDP-43-positive neuronal inclusions (H). The corticospinal tract showed mild

myelin pallor (F). In a patient with type C pathological change, the frontal and temporal cortices showed severe atrophy (I), marked neuronal loss (K), and pTDP-43-positive long dystrophic neurites (L). The corticospinal tract showed marked myelin pallor (J). Klüver-Barrera staining (A, B, E, F, I, and J), hematoxylin-eosin staining (C, G, and K), and pTDP-43 immunohistochemistry (D, H, and L) were performed. Scale bars represent 1 cm (A, E, and I), 3 mm (B, F, and J), 100  $\mu$ m (C, G, and K), and 20  $\mu$ m (D, H, and L). Original magnifications are  $\times 1$  (A, B, E, F, I, and J),  $\times 200$  (C, G, and K), and  $\times 400$  (D, H, and L).

#### Anti-UBQLN-2 and Anti-p62N Immunohistochemistry

No patients showed any cerebellar UBQLN-2-positive or p62N-positive structures. In the temporal lobes, UBQLN-2-positive structures were occasionally observed in 8 patients, but abundant, thick, and aggregatelike structures, which are found in patients with C9ORF72 expansions, were not observed (eFigure 3 in Supplement). We presumed that our patients did not have C9ORF72 expansions.

#### Discussion

Our study demonstrated that pTDP-43-associated pathological changes were common in the spinal anterior horns of the FTLT without ALS, FTLT-ALS, and ALS-FTLT groups. Neuronal loss and gliosis were most severe among the ALS-FTLT group, followed by the FTLT-ALS and then the FTLT without ALS groups. Our results clearly demonstrated the pathological continuum among TDP-43-associated FTLT and ALS, even at the LMN level.

Although the FTLT without ALS group that lacked LMN symptoms showed a loss of LMNs, the degree of neuronal loss and TDP-43 disease were generally mild in this group. Experiment data using ALS mouse models revealed that symptoms developed when approximately 29% of spinal motor neurons were lost.<sup>25</sup> Further investigation will be needed to clarify whether LMN involvement occurs in a later stage of illness or progresses very slowly compared with cerebral involvement in FTLT without ALS.

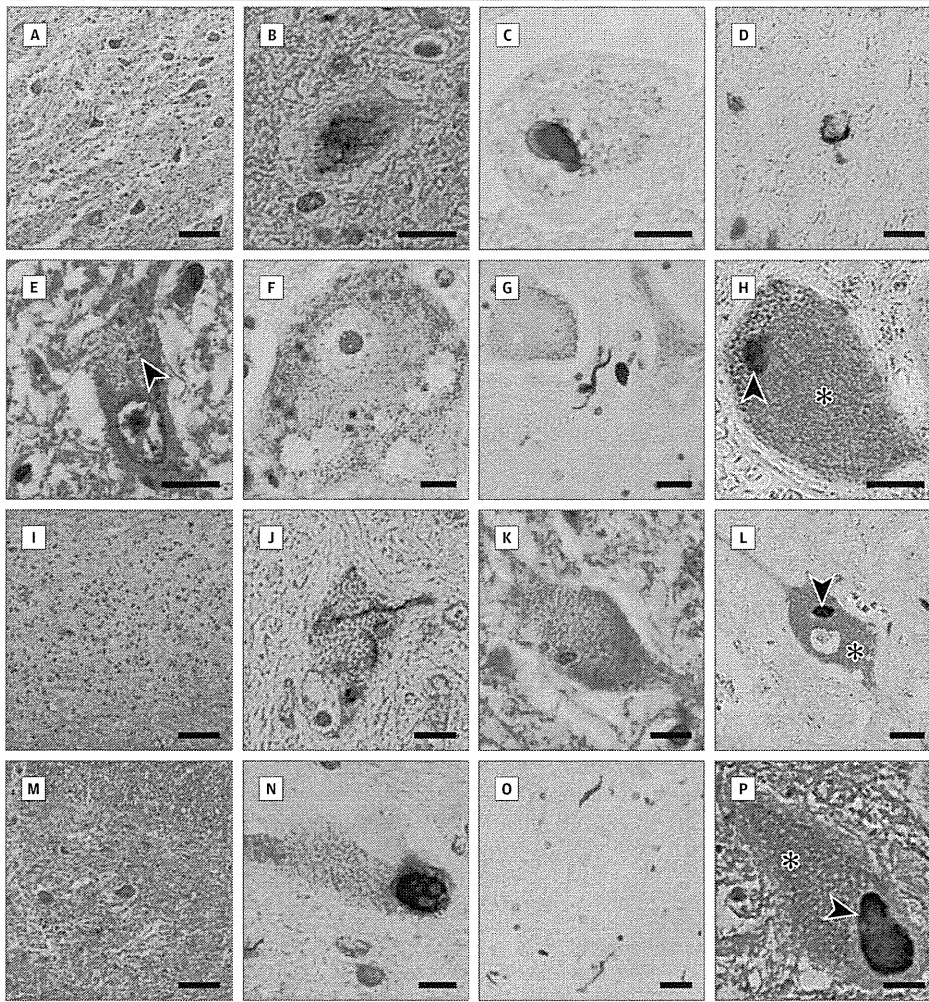
Our results revealed that the FTLT-TDP types A, B, and C were associated with neuropathological changes corresponding to ALS in the spinal motor neurons. The severity of neuronal loss and pTDP-43 disease in the spinal motor neurons

may differ quantitatively among these neuropathological subtypes. Based on cortical TDP-43 pathological findings, patients in the type B group had severe neuronal loss and diffuse pTDP-43-positive neuronal inclusions, which were entirely identical to ALS, whereas these changes were mild in the type C group. In type A, LMN pathological findings were diverse regardless of clinical duration; their severity and extension may be heterogeneous among patients with type A disease, unlike those with type B or C disease. Indeed, type A disease has also been identified in the FTLT with ALS phenotype in sporadic or familial (C9ORF72 expansion or progranulin gene mutations) form.<sup>2,5,21,26</sup> Dystrophic neurites were prominent in the spinal anterior horn of patients with type A or C disease. In our patient series, Bunina bodies were observed in most patients with type A or B disease but were absent in those with type C disease, findings consistent with those of previous studies.<sup>3,17</sup>

Several studies have demonstrated that some patients with FTLT-TDP, particularly type C, showed marked CST degeneration.<sup>3,11,17,27</sup> We also observed a marked myelin pallor in the CST in 67% of patients with FTLT without ALS, 12% with FTLT-ALS, and 16% with ALS-FTLT (50% for type A, 15% for type B, and 100% for type C). Some patients showed neuronal loss or gliosis in the primary motor cortex to varying extents. Furthermore, patients with FTLT without ALS often exhibited severe degenerative changes in broad areas of the frontal cortices. The broad involvement of the frontal lobes might also contribute to the CST degeneration because CST fibers arise not only from the primary motor cortex but also from the premotor cortex and supplementary motor areas.<sup>28</sup>

Two limitations of our study is that the evaluation of slight or very mild muscle weakness was not completed and that there were few patients with electromyographic data in

Figure 4. Pathological Findings of Spinal Motor Neuron in Subtypes of TAR DNA-Binding Protein of 43 kDa (TDP-43) Pathological Changes



Patients with type A (A-H), type B (I-L), and type C (M-P) pathological changes. A patient with type A pathological change showed mild neuronal loss (A), phosphorylated TDP-43 (pTDP-43)-positive skeinlike cytoplasmic inclusions (B), nuclear inclusions (C), and glial inclusions (D), Bunina bodies (E [arrow] and F) in the spinal anterior horn, and dystrophic neurites (G). In a patient with type B pathological change, neuronal loss (I), pTDP-43-positive skeinlike cytoplasmic inclusions (J), and Bunina bodies (K) were markedly observed. In a patient with type C pathological change, the spinal anterior horn showed mild neuronal loss (M), pTDP-43-positive skeinlike cytoplasmic inclusions (N), and dystrophic neurites (O). Double immunohistochemistry for choline acetyltransferase (ChAT) and pTDP-43 revealed cytoplasmic inclusions (violet [arrows]) present within the cytoplasm of a ChAT-positive spinal motor neuron (brown [asterisks]) of patients with type A (H), B (L), or C (P) pathological change. Hematoxylin-eosin staining (A, E, I, K, and M), pTDP-43 immunohistochemistry (B, C, D, G, J, N, and O), cystatin-C (F), and double immunohistochemical analysis for pTDP-43 and ChAT (H, L, and P) were performed. Scale bars represent 100 (A, I, and M), 20 (G, L, and O), and 10 (B-F, H, J, K, N, and P)  $\mu\text{m}$ . Original magnifications are  $\times 100$  (A, I, and M),  $\times 400$  (G, L, and O), and  $\times 1000$  (B-F, H, J, K, N, and P).

the FTLN without ALS group. However, our clinical data demonstrated that patients with FTLN without ALS had significantly longer survival times than those with FTLN-ALS or ALS-FTLN. These prognostic data correspond well to previous results.<sup>29,30</sup> In addition, the causes of death differed considerably between the FTLN without ALS group and the FTLN-ALS and ALS-FTLN groups. Respiratory failure was observed in patients with FTLN-ALS or ALS-FTLN but not in those with FTLN without ALS, and respiratory failure was

strongly associated with severity of LMN loss. These results support the view that classification of FTLN based on the presence of LMN involvement was applicable in this study.

In conclusion, the LMN systems of FTLN-TDP generally show neuropathological changes that are indicative of ALS, although the severity of pathological changes differs among clinical phenotypes or subtypes of cortical TDP-43 disease. A pathological continuity between FTLN-TDP and ALS is supported by evidence of LMN involvement.

#### ARTICLE INFORMATION

**Accepted for Publication:** October 16, 2013.

**Published Online:** December 30, 2013.  
doi:10.1001/jamaneurol.2013.5489.

**Author Contributions:** Drs Sobue and Yoshida had full access to all the data in the study and take responsibility for the integrity of the data and the accuracy of the data analysis.  
*Study concept and design:* Riku, Watanabe, Yoshida, Sobue.

*Acquisition of data:* Riku, Watanabe, Yoshida, Masuda, Senda, Sobue.

*Analysis and interpretation of data:* Riku, Watanabe,

Yoshida, Tatsumi, Mimuro, Iwasaki, Katsuno, Iguchi, Ishigaki, Udagawa, Sobue.

*Drafting of the manuscript:* Riku, Watanabe, Yoshida, Sobue.

*Critical revision of the manuscript for important intellectual content:* Tatsumi, Mimuro, Iwasaki, Katsuno, Iguchi, Masuda, Senda, Ishigaki, Udagawa, Sobue.

*Statistical analysis:* Riku, Watanabe, Masuda, Senda.

*Administrative, technical, or material support:* Riku, Yoshida, Tatsumi, Mimuro, Iwasaki, Iguchi, Udagawa.

*Study supervision:* Watanabe, Yoshida, Katsuno, Senda, Sobue.

**Conflict of Interest Disclosures:** None reported.

**Funding/Support:** This work was supported by grants-in-aid from the Research Committee of Central Nervous System Degenerative Diseases by Ministry of Health, Labour, and Welfare and from Integrated Research on Neuropsychiatric Disorders, carried out under the Strategic Research for Brain Sciences by Ministry of Education, Culture, Sports, Science, and Technology of Japan.

**Role of the Sponsor:** The funding agencies had no role in the design and conduct of the study; collection, management, analysis, and interpretation of the data; preparation, review, or approval of the manuscript; and decision to submit the manuscript for publication.

**Additional Contributions:** We thank all the patients, their families, and the staff in the affiliated hospitals for providing autopsy materials and clinical data.

## REFERENCES

- Cairns NJ, Neumann M, Bigio EH, et al. TDP-43 in familial and sporadic frontotemporal lobar degeneration with ubiquitin inclusions. *Am J Pathol*. 2007;171(1):227-240.
- Josephs KA, Whitwell JL, Murray ME, et al. Corticospinal tract degeneration associated with TDP-43 type C pathology and semantic dementia. *Brain*. 2013;136(pt 2):455-470.
- Mackenzie IR, Neumann M, Bigio EH, et al. Nomenclature and nosology for neuropathologic subtypes of frontotemporal lobar degeneration: an update. *Acta Neuropathol*. 2010;119(1):1-4.
- Whitwell JL, Jack CR Jr, Parisi JE, et al. Does TDP-43 type confer a distinct pattern of atrophy in frontotemporal lobar degeneration? *Neurology*. 2010;75(24):2212-2220.
- Mackenzie IR, Neumann M, Baborie A, et al. A harmonized classification system for FTL-D-TDP pathology. *Acta Neuropathol*. 2011;122(1):111-113.
- Mackenzie IR, Baborie A, Pickering-Brown S, et al. Heterogeneity of ubiquitin pathology in frontotemporal lobar degeneration: classification and relation to clinical phenotype. *Acta Neuropathol*. 2006;112(5):539-549.
- Sampathu DM, Neumann M, Kwong LK, et al. Pathological heterogeneity of frontotemporal lobar degeneration with ubiquitin-positive inclusions delineated by ubiquitin immunohistochemistry and novel monoclonal antibodies. *Am J Pathol*. 2006;169(4):1343-1352.
- Neumann M, Sampathu DM, Kwong LK, et al. Ubiquitinated TDP-43 in frontotemporal lobar degeneration and amyotrophic lateral sclerosis. *Science*. 2006;314(5796):130-133.
- Josephs KA, Dickson DW. Frontotemporal lobar degeneration with upper motor neuron disease/primary lateral sclerosis. *Neurology*. 2007;69(18):1800-1801.
- Geser F, Lee VM, Trojanowski JQ. Amyotrophic lateral sclerosis and frontotemporal lobar degeneration: a spectrum of TDP-43 proteinopathies. *Neuropathology*. 2010;30(2):103-112.
- Snowden J, Neary D, Mann D. Frontotemporal lobar degeneration: clinical and pathological relationships. *Acta Neuropathol*. 2007;114(1):31-38.
- Geser F, Martinez-Lage M, Robinson J, et al. Clinical and pathological continuum of multisystem TDP-43 proteinopathies. *Arch Neurol*. 2009;66(2):180-189.
- Nishihira Y, Tan CF, Hoshi Y, et al. Sporadic amyotrophic lateral sclerosis of long duration is associated with relatively mild TDP-43 pathology. *Acta Neuropathol*. 2009;117(1):45-53.
- Geser F, Stein B, Partain M, et al. Motor neuron disease clinically limited to the lower motor neuron is a diffuse TDP-43 proteinopathy. *Acta Neuropathol*. 2011;121(4):509-517.
- Yoshida M. Amyotrophic lateral sclerosis with dementia: the clinicopathological spectrum. *Neuropathology*. 2004;24(1):87-102.
- Kobayashi Z, Tsuchiya K, Arai T, et al. Clinicopathological characteristics of FTL-D-TDP showing corticospinal tract degeneration but lacking lower motor neuron loss. *J Neurol Sci*. 2010;298(1-2):70-77.
- Brooks BR, Miller RG, Swash M, Munsat TL; World Federation of Neurology Research Group on Motor Neuron Diseases. El Escorial revisited: revised criteria for the diagnosis of amyotrophic lateral sclerosis. *Amyotroph Lateral Scler Other Motor Neuron Disord*. 2000;1(5):293-299.
- Neary D, Snowden JS, Gustafson L, et al. Frontotemporal lobar degeneration: a consensus on clinical diagnostic criteria. *Neurology*. 1998;51(6):1546-1554.
- Braak H, Alafuzoff I, Arzberger T, Kretschmar H, Del Tredici K. Staging of Alzheimer disease-associated neurofibrillary pathology using paraffin sections and immunocytochemistry. *Acta Neuropathol*. 2006;112(4):389-404.
- Simón-Sánchez J, Doppler EG, Cohn-Hokke PE, et al. The clinical and pathological phenotype of C9ORF72 hexanucleotide repeat expansions. *Brain*. 2012;135(pt 3):723-735.
- Murray ME, DeJesus-Hernandez M, Rutherford NJ, et al. Clinical and neuropathologic heterogeneity of c9FTD/ALS associated with hexanucleotide repeat expansion in C9ORF72. *Acta Neuropathol*. 2011;122(6):673-690.
- Konno T, Shiga A, Tsujino A, et al. Japanese amyotrophic lateral sclerosis patients with GGGGCC hexanucleotide repeat expansion in C9ORF72. *J Neurol Neurosurg Psychiatry*. 2013;84(4):398-401.
- Brettschneider J, Van Deerlin VM, Robinson JL, et al. Pattern of ubiquitin pathology in ALS and FTL-D indicates presence of C9ORF72 hexanucleotide expansion. *Acta Neuropathol*. 2012;123(6):825-839.
- Pringle CE, Hudson AJ, Munoz DG, Kiernan JA, Brown WF, Ebers GC. Primary lateral sclerosis. Clinical features, neuropathology and diagnostic criteria. *Brain*. 1992;115(pt 2):495-520.
- Morrison BM, Janssen WG, Gordon JW, Morrison JH. Time course of neuropathology in the spinal cord of G86R superoxide dismutase transgenic mice. *J Comp Neurol*. 1998;391(1):64-77.
- Baker M, Mackenzie IR, Pickering-Brown SM, et al. Mutations in progranulin cause tau-negative frontotemporal dementia linked to chromosome 17. *Nature*. 2006;442(7105):916-919.
- Yokota O, Tsuchiya K, Arai T, et al. Clinicopathological characterization of Pick's disease versus frontotemporal lobar degeneration with ubiquitin/TDP-43-positive inclusions. *Acta Neuropathol*. 2009;117(4):429-444.
- Standing S, ed. *Gray's Anatomy: The Anatomical Basis of Clinical Practice*. 39th edition. London, England: Churchill Livingstone; 2004.
- Josephs KA, Knopman DS, Whitwell JL, et al. Survival in two variants of tau-negative frontotemporal lobar degeneration: FTL-D vs FTL-D-MND. *Neurology*. 2005;65(4):645-647.
- Hodges JR, Davies R, Xuereb J, Kril J, Halliday G. Survival in frontotemporal dementia. *Neurology*. 2003;61(3):349-354.

## *ERBB4* Mutations that Disrupt the Neuregulin-ErbB4 Pathway Cause Amyotrophic Lateral Sclerosis Type 19

Yuji Takahashi,<sup>1</sup> Yoko Fukuda,<sup>1</sup> Jun Yoshimura,<sup>2</sup> Atsushi Toyoda,<sup>3</sup> Kari Kurppa,<sup>4,5</sup> Hiroyoko Moritoyo,<sup>6</sup> Veronique V. Belzil,<sup>7</sup> Patrick A. Dion,<sup>7,8</sup> Koichiro Higasa,<sup>2</sup> Koichiro Doi,<sup>2</sup> Hiroyuki Ishiura,<sup>1</sup> Jun Mitsui,<sup>1</sup> Hidetoshi Date,<sup>1</sup> Budrul Ahsan,<sup>1</sup> Takashi Matsukawa,<sup>1</sup> Yaeko Ichikawa,<sup>1</sup> Takashi Moritoyo,<sup>6</sup> Mayumi Ikoma,<sup>9</sup> Tsukasa Hashimoto,<sup>9</sup> Fumiharu Kimura,<sup>10</sup> Shigeo Murayama,<sup>11</sup> Osamu Onodera,<sup>12</sup> Masatoyo Nishizawa,<sup>12</sup> Mari Yoshida,<sup>13</sup> Naoki Atsuta,<sup>14</sup> Gen Sobue,<sup>14</sup> JaCALS,<sup>15</sup> Jennifer A. Fifita,<sup>16,17,18</sup> Kelly L. Williams,<sup>16,17,18</sup> Ian P. Blair,<sup>16,17,18</sup> Garth A. Nicholson,<sup>16,17</sup> Paloma Gonzalez-Perez,<sup>19</sup> Robert H. Brown, Jr.,<sup>19</sup> Masahiro Nomoto,<sup>6</sup> Klaus Elenius,<sup>4,20</sup> Guy A. Rouleau,<sup>7,21,22</sup> Asao Fujiyama,<sup>3</sup> Shinichi Morishita,<sup>2</sup> Jun Goto,<sup>1</sup> and Shoji Tsuji<sup>1,23,\*</sup>

Amyotrophic lateral sclerosis (ALS) is a devastating neurological disorder characterized by the degeneration of motor neurons and typically results in death within 3–5 years from onset. Familial ALS (FALS) comprises 5%–10% of ALS cases, and the identification of genes associated with FALS is indispensable to elucidating the molecular pathogenesis. We identified a Japanese family affected by late-onset, autosomal-dominant ALS in which mutations in genes known to be associated with FALS were excluded. A whole-genome sequencing and parametric linkage analysis under the assumption of an autosomal-dominant mode of inheritance with incomplete penetrance revealed the mutation c.2780G>A (p. Arg927Gln) in *ERBB4*. An extensive mutational analysis revealed the same mutation in a Canadian individual with familial ALS and a de novo mutation, c.3823C>T (p. Arg1275Trp), in a Japanese simplex case. These amino acid substitutions involve amino acids highly conserved among species, are predicted as probably damaging, and are located within a tyrosine kinase domain (p. Arg927Gln) or a C-terminal domain (p. Arg1275Trp), both of which mediate essential functions of ErbB4 as a receptor tyrosine kinase. Functional analysis revealed that these mutations led to a reduced autophosphorylation of ErbB4 upon neuregulin-1 (NRG-1) stimulation. Clinical presentations of the individuals with mutations were characterized by the involvement of both upper and lower motor neurons, a lack of obvious cognitive dysfunction, and relatively slow progression. This study indicates that disruption of the neuregulin-ErbB4 pathway is involved in the pathogenesis of ALS and potentially paves the way for the development of innovative therapeutic strategies such as using NRGs or their agonists to upregulate ErbB4 functions.

Amyotrophic lateral sclerosis (ALS) is a devastating neurological disorder in which the degeneration of motor neurons leads to progressive weakness and wasting of limb, bulbar, and respiratory muscles. Familial ALS (FALS) comprises 5%–10% of ALS cases, and the remaining cases are simplex cases of ALS (SALS). To date, more than 20 genes have been shown to be associated with ALS,<sup>1</sup> and these account for 75% of FALS and 14% of SALS cases.<sup>2</sup> Mutations that are found in FALS-associated genes but that are also identified in individuals with SALS are considered mutations with reduced penetrance or de novo mutations. Further discovery of genes associated with FALS is indispensable

to elucidating the molecular backgrounds of both FALS and SALS.

Identification of genes associated with familial diseases has been accomplished through identification of the disease loci on the chromosomes by linkage analysis of large pedigrees and subsequent positional cloning of the genes. The majority of the FALS pedigrees, however, are not large and do not have multiple affected members as a result of the poor prognosis of the disease and the late age of onset, which makes it difficult to sufficiently narrow the candidate regions by linkage analyses and means that it takes a tremendous effort to identify the genes associated with FALS. The recent development of massively parallel

<sup>1</sup>Department of Neurology, Graduate School of Medicine, The University of Tokyo, Tokyo 113-8655, Japan; <sup>2</sup>Department of Computational Biology, Graduate School of Frontier Sciences, The University of Tokyo, Chiba 277-8561, Japan; <sup>3</sup>Comparative Genomics Laboratory, National Institute of Genetics, Shizuoka 411-8540, Japan; <sup>4</sup>Department of Medical Biochemistry and Genetics, University of Turku, Turku, 20014, Finland; <sup>5</sup>Turku Doctoral Programme of Biomedical Sciences, Turku, 20520, Finland; <sup>6</sup>Department of Neurology and Clinical Pharmacology, Ehime University Hospital, Ehime 791-0295, Japan; <sup>7</sup>Research Center, Centre Hospitalier Universitaire Sainte-Justine, Université de Montréal, Montréal, QC, H3T 1C5, Canada; <sup>8</sup>Department of Pathology and Cellular Biology, Université de Montréal, Montréal, QC H3T 1C5, Canada; <sup>9</sup>Department of Neurology, National Hospital Organization Ehime National Hospital, Ehime 791-0281, Japan; <sup>10</sup>Division of Neurology, First Department of Internal Medicine, Osaka Medical College, Osaka 569-8686, Japan; <sup>11</sup>Department of Neurology and Neuropathology and Brain Bank for Aging Research, Tokyo Metropolitan Geriatric Hospital and Institute of Gerontology, Tokyo 173-0015, Japan; <sup>12</sup>Department of Neurology, Brain Research Institute, Niigata University, Niigata 951-8520, Japan; <sup>13</sup>Department of Neuropathology, Institute for Medical Science of Aging, Aichi Medical University, Aichi 480-1195, Japan; <sup>14</sup>Department of Neurology, Nagoya University Graduate School of Medicine, Nagoya 466-8560, Japan; <sup>15</sup>Japanese Consortium for Amyotrophic Lateral Sclerosis Research; <sup>16</sup>Northcott Neuroscience Laboratory, ANZAC Research Institute, Sydney, New South Wales 2139, Australia; <sup>17</sup>Sydney Medical School, University of Sydney, New South Wales 2006, Australia; <sup>18</sup>Austrian School of Medicine, Macquarie University, Sydney, New South Wales 2109, Australia; <sup>19</sup>Department of Neurology, University of Massachusetts Medical School, Worcester, MA 01655-0318, USA; <sup>20</sup>Department of Oncology, Turku University Hospital, Turku 20521, Finland; <sup>21</sup>Montreal Neurological Institute, McGill University, Montreal, QC H3A 2B4, Canada; <sup>22</sup>Department of Neurology and Neurosurgery, McGill University, Montreal, QC H3A 2B4, Canada; <sup>23</sup>Medical Genome Center, The University of Tokyo Hospital, The University of Tokyo, Tokyo 113-8655, Japan

\*Correspondence: [tsuji@m.u-tokyo.ac.jp](mailto:tsuji@m.u-tokyo.ac.jp)

<http://dx.doi.org/10.1016/j.ajhg.2013.09.008>. ©2013 by The American Society of Human Genetics. All rights reserved.

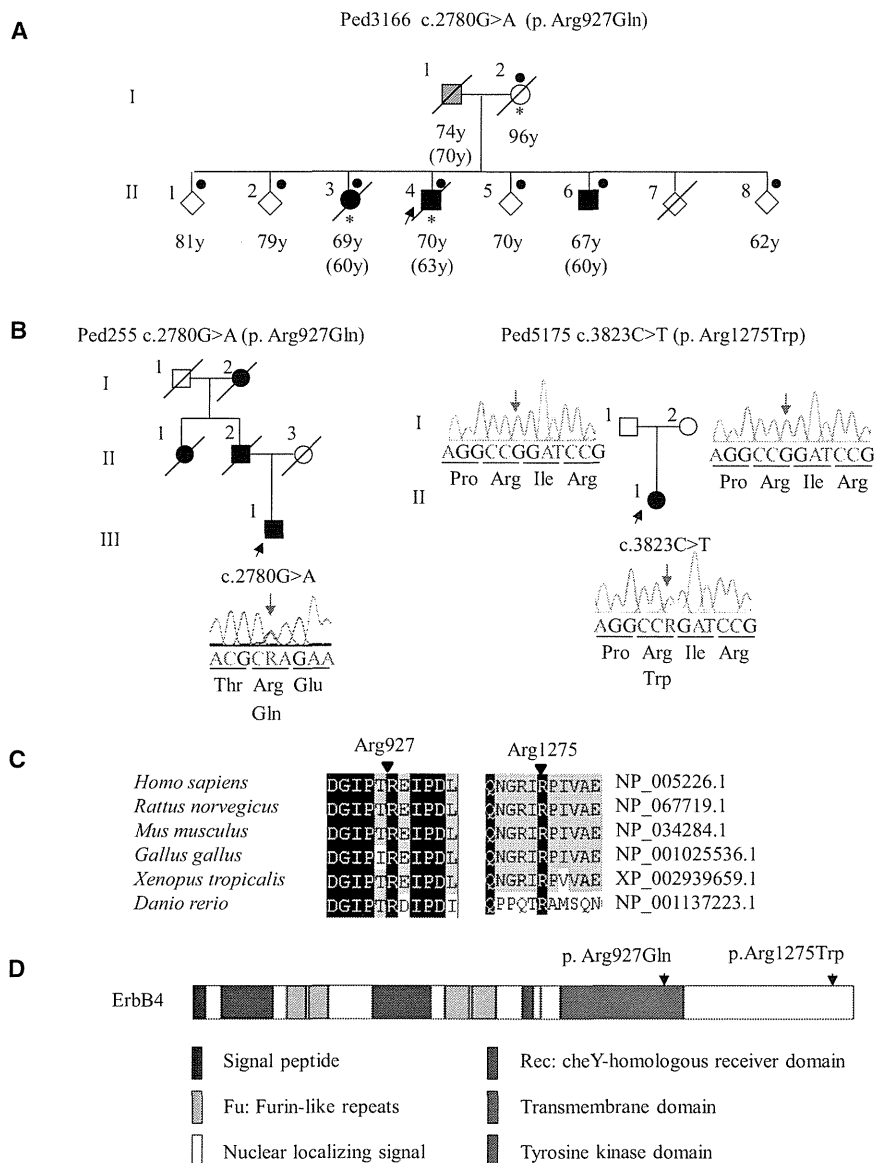


**Figure 1. Pedigrees of ALS and Characterization of Mutations**

(A) Pedigree charts of the index family. Filled symbols indicate affected individuals. The arrow indicates the proband. For confidentiality purposes, all unaffected siblings are indicated by diamonds. Dots or asterisks indicate individuals included in the linkage study or WGS, respectively. Age at present or age at death is shown under each individual, and ages at onset are shown in parentheses. The box with gray shading indicates that the individual's clinical information obtained from the family members strongly supports the diagnosis of ALS, although detailed neurological evaluations have not been conducted for this individual.

(B) Additional Canadian (Ped255) and Japanese (Ped5175) pedigrees with *ERBB4* mutations. The electropherograms of mutational data are shown beside each member. Nucleotide colors correspond to the colors in the electropherograms. The amino acids are designated below the nucleotide sequences. The blue arrows indicate the nucleotide positions of the mutations. In the electropherograms (Ped5175), nucleotide sequences of the reverse complementary strand are shown.

(C) Amino acid conservation. The amino acids Arg927 and Arg1275 are highly conserved among species.

(D) The protein structure along with the locations of amino acid substitutions are shown; amino acid substitutions are indicated by arrows. The amino acid substitution p. Arg927Gln resides in the tyrosine kinase domain, which mediates the key functions of ErbB4. The amino acid substitution p. Arg1275Trp resides in the C-terminal domain in the vicinity of multiple phosphorylation sites, which mediate downstream signaling pathways.

sequencing technologies has allowed us to overcome the difficulty by means of whole-genome sequencing (WGS) or exome analysis.

We identified a Japanese family with three affected siblings presenting with late-onset ALS (Figure 1A and Table 1). The familial history indicated that the mode of inheritance is probably an autosomal-dominant one. Mutational analysis of the proband (II-4) employing direct nucleotide sequence analysis, a microarray-based resequencing, or a repeat-primed PCR analysis excluded *SOD1*[MIM 147450], *ALS2*[MIM 606352], *DCTN1*[MIM 601143], *CHMP2B*[MIM 609512], *ANG*[MIM 105850], *TARDBP*[MIM 605078], *FUS*[MIM 137070] and *C9ORF72* [MIM 1614260] as the genes associated with FALS.<sup>3,4</sup> To identify a gene associated with FALS, we applied WGS in combination with a linkage analysis to the pedigree. Written informed consent was obtained from all the participants. This study was approved by the institutional review board at the University of Tokyo.

WGS was performed on three individuals (I-2, II-3 and II-4, as shown in Figure 1A) in the index pedigree. Paired-end DNA libraries were generated and subjected to massively parallel sequencing with a GAII Illumina Genome Analyzer in accordance with the manufacturer's instructions. The short read sequences obtained were aligned to the reference genome (NCBI37/hg19 assembly) via the Burrows-Wheeler Aligner.<sup>5</sup> Downstream analyses in which potential PCR duplicates were removed were processed with SAMtools.<sup>6</sup> Aligned reads were viewed on an Integrative Genomics Viewer.<sup>7</sup> Genomic sequence variations were identified with the SAMtools pileup command and annotated with Refseq, dbSNP135, 1000 Genomes, personal genome databases, the NHLBI GO Exome Sequencing Project (NHLBI-ESP) database, and an in-house variant database containing 41 whole genomes and 1,408 exomes in the Japanese population. The numbers of non-synonymous variants that were identified in individuals I-2, II-3, and II-4 but that were not present in any of the

**Table 1. Clinical Characteristics of Affected Individuals**

Pedigree Number	Pedigree 3166				Pedigree 255	Pedigree 5175
Ethnicity	Japanese				Canadian	Japanese
Inheritance	familial (autosomal dominant)				familial (autosomal dominant)	simplex
Mutation	c.2780G>A				c.2780G>A	c.3823C>T
Amino acid substitution	p. Arg927Gln				p. Arg927Gln	p. Arg1275Trp
Members	I-1	II-3	II-4 (proband)	II-6	III-3	II-1
Age at onset	70	60	63	60	67	45
Initial symptoms	bulbar	N.D.	upper limbs	respiration	upper limbs	upper limbs
Diagnostic criteria <sup>a</sup>	N.D.	N.D.	definite	definite	probable	probable
Progression	unable to walk after 3 years	ventilator -dependent after 5 years, locked-in state after 8 years	locked-in state after 5 years	ventilator- dependent after 1 year, locked-in state after 5 years	slow progression that significantly decelerated and finally stopped after 8 years	wheelchair- bound, MRS 1-2/5 in upper extremities after 5 years
Cognitive function	N.D.	N.D.	normal	normal	N.D.	normal
Age at death	74	69	70	66	N/A	N/A

Abbreviations are as follows: N.D., not described; MRS, manual muscle testing rating scale; and N/A, not applicable.

<sup>a</sup>El Escorial and Airlie House revised criteria.

databases (hereafter, variants not found in the databases are referred to as “novel”) were 411, 404, and 382, respectively (Table S1). No novel nonsynonymous variants in genes known to be associated with FALS were included. Among the identified variants, 57 were identified both in the proband and in the affected sibling, but not in the mother, and were subjected to further analysis.

The individuals indicated by dots in Figure 1A were genotyped with Genome-Wide Human SNP Array 6.0 (Affymetrix). Linkage analysis and haplotype reconstruction were conducted with the pipeline software SNP-HiTLink<sup>8</sup> and Allegro version 2<sup>9</sup> under the assumption of an autosomal-dominant mode of inheritance and a disease-allele frequency of 0.000001. Parametric multipoint linkage analysis under the assumption of complete penetrance revealed three loci spanning 23.6 Mb on chromosomes 1, 6, and 13, having a maximum LOD score of 1.8 (Figure S1; penetrance = 1.0), and containing 88 annotated genes. However, no novel nonsynonymous variants were identified in the candidate regions. We then considered the possibility of reduced penetrance. When penetrance was reduced to 0.8 (Figure S1), seven additional loci had LOD scores > 0.7 and were thus shown to support linkage; these loci contained 809 annotated genes. Three heterozygous novel nonsynonymous variants were identified in these regions; among these variants, only c.2780G>A (p. Arg927Gln; dbSNP SubSNP ID ss831884245) substituting glutamine for arginine at codon 927 (p. Arg927Gln) in *v-erb-a* erythroblastic leukemia viral oncogene homolog 4 (avian) (*ERBB4* [MIM 600543; RefSeq accession number NM\_005235.2]) was not present in 477 controls (Table S2). When we allowed further reduced penetrance, we identified 19 additional loci with LOD > 0; these loci con-

tained 1,265 annotated genes. In these regions, we identified seven heterozygous novel nonsynonymous variants, among which three variants in *OR2D3* (RefSeq NM\_001004684.1), *FTCD* (MIM 606806; RefSeq NM\_206965.1), and *TJP2* (MIM 607709; RefSeq NM\_001170414.2) were not present in 477 controls (Table S2). *OR2D3* is an olfactory receptor gene; the substituted amino acid in *OR2D3* is not conserved, and the substitution is predicted as benign by PolyPhen-2 analysis. *FTCD* and *TJP2* are associated with autosomal-recessive glutamate formiminotransferase deficiency (MIM 229100) and familial hypercholanemia (MIM 607748), respectively, and heterozygous carriers have not been described as exhibiting ALS. Taken together, the results pointed to c.2780G>A in *ERBB4* as the most likely pathogenic mutation.

We used a direct nucleotide sequence analysis method to conduct mutational analysis of *ERBB4* in 364 FALS and 818 SALS individuals by using an ABI 3100 sequencer and BigDye Terminator ver3.1 (Applied Biosystems). We used the ExonPrimer website to design oligonucleotide primers (Table S3). The mutation c.2780G>A was also identified in one Canadian FALS individual (Figure 1B). Unfortunately, DNA from other family members was not available to confirm segregation. To investigate a possibility that the c.2780G>A mutation identified in the Japanese and Canadian families is a common founder mutation, we compared the haplotypes with the c.2780G>A mutation in *ERBB4* of the Japanese and Canadian families (Figure S2). Different SNPs were observed 14 kbp and 5 kbp centromeric and telomeric to the mutation, respectively, indicating that disease haplotypes of the Japanese and Canadian families are different and that

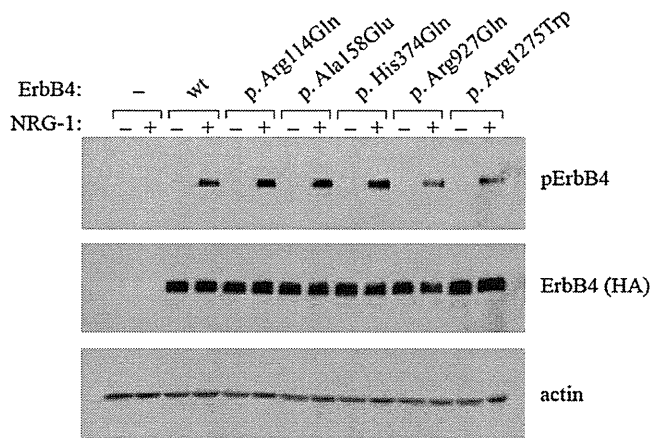


**Figure 2. Functional Analysis of Wild-Type and Mutant ErbB4 upon Neuregulin-1 Stimulation**

COS-7 cells transfected with an empty-vector control or plasmids encoding either wild-type (wt) or mutant HA-tagged ErbB4 (p. Arg114Gln, p. Ala158Glu, p. His374Gln, p. Arg927Gln, or p. Arg1275Trp) were stimulated with or without NRG-1, and the autophosphorylation activity of ErbB4 was analyzed by immunoblot analysis with antibodies against phospho-ErbB4 (Tyr1284) (Cell Signaling) and HA tag (Abcam), respectively. For loading controls, immunoblotting was performed with an anti-actin antibody (Santa Cruz Biotechnology). Three amino acid substitutions, including p.Arg114Gln, p.Ala158Glu, and p.His374Gln (rs760369), identified through mutational analysis of FALS and SALS individuals, were included in autophosphorylation assay. The substitutions p.Arg114Gln and p.Ala158Glu were not considered to be relevant to ALS because neither recurrence nor cosegregation was confirmed.

mutation occurred independently. We identified a de novo mutation of c.3823C>T (dbSNP SubSNP ID ss831884246), substituting tryptophan for arginine at codon 1275 (p. Arg1275Trp), in a Japanese SALS individual (Figure 1B) in whom a biological parent-descendant relationship was confirmed (Table S4) by the PLINK<sup>10</sup> algorithm. These mutations were neither present in the 477 Japanese controls nor registered in the in-house database containing 41 whole genomes and 1408 exomes, the 1000 Genomes database, or the NHLBI-ESP database, containing 6503 exomes. Furthermore, c.2780G>A was not present in 190 Canadian controls. The identification of c.2780G>A in two independent families of different ethnic backgrounds strongly supported c.2780G>A as the causative mutation for ALS. Given that de novo mutation rates have been estimated to be  $1.20 \times 10^{-8}$  per nucleotide per generation<sup>11</sup> and less than one nonsynonymous single-nucleotide variant (SNV)/generation,<sup>12</sup> the observation of the de novo mutation further supports the idea that c.3823C>T is likely to be the causative mutation for ALS in this individual. The mutation's substituted arginine residues, Arg927 and Arg1275, are highly conserved among species (Figure 1C), and the substitutions are predicted to be probably damaging by PolyPhen-2 analysis. The amino acid residue Arg927 resides in a tyrosine kinase domain, which is essential for the receptor tyrosine kinase activity, and Arg1275 is located in a C-terminal domain in the vicinity

of multiple phosphorylation sites, which mediate downstream signaling pathways (Figure 1D). The clinical presentations of these ALS individuals with the *ERBB4* mutations are summarized in Table 1. The common clinical characteristics of the individuals included both upper and lower motor-neuron involvement diagnosed as definite or probable ALS according to El Escorial and Airlie House revised criteria, relatively slow disease progression, and no obvious cognitive impairment. The individuals with the c.2780G>A mutation were characterized by relatively late onset (the ages at onset ranged from 60–70 years) and a slightly reduced penetrance. In contrast, the individual with the c.3823C>T mutation was characterized by early onset (45 years of age).

ErbB4 is a member of the epidermal growth factor (EGF) subfamily of receptor tyrosine kinases (RTKs). It forms a homodimer or a heterodimer with ErbB2 or ErbB3 and is activated upon binding of neuregulins (NRGs) to the extracellular ligand-binding domain of ErbB4.<sup>13</sup> Activation of ErbB4 is mediated by increased tyrosine kinase activity upon NRG binding, resulting in autophosphorylation of the C-terminal tail.<sup>14</sup> To determine how the two mutations identified in the ALS individuals affect ErbB4 functions, we investigated the autophosphorylation of ErbB4 in cells expressing either wild-type or mutant (c.2780G>A or c.3823C>T) *ERBB4* in the presence of NRG-1. The *ERBB4* mutations were introduced into the pBAGE-pur-o*ERBB4*JM-aCYT-2HA plasmid encoding HA-tagged ErbB4 JM-a CYT-2<sup>15</sup> by site-directed mutagenesis according to the protocol described in the Phusion Site-Directed Mutagenesis Kit (Thermo Fisher Scientific). After mutagenesis, all the constructs were verified by sequencing. The plasmids were transiently transfected into COS-7 cells via FuGENE 6 transfection reagent (Roche) in accordance with the manufacturer's instructions. Transfected cells were starved of serum overnight and stimulated with 0 or 50 ng/ml NRG-1 (R&D Systems) for 10 min at 37°C. After stimulation, the cells were lysed, and samples equivalent to 50 µg of total protein were separated through 8% SDS-PAGE gels. For detection of ErbB4 phosphorylation and total ErbB4 protein levels, immunoblotting was performed with antibodies against phospho-ErbB4 (Tyr1284) (Cell Signaling) and HA-tag (Abcam), respectively. The two amino acid substitutions, p. Arg927Gln and p. Arg1275Trp, showed a clearly reduced autophosphorylation of ErbB4 (Figure 2). On the basis of these genetic and functional data, we concluded that the two mutations are causative mutations for ALS (ALS19).

This study revealed that a reduced autophosphorylation of ErbB4 upon NRG-1 stimulation is involved in the pathogenesis of ALS. *ErbB4* is specifically expressed in the soma of large motor neurons of the rat spinal cord.<sup>16</sup> The lack of *ErbB4* is embryonically lethal in mice, which displayed the derangement of motor-neuron axon guidance and pathfinding during embryogenesis.<sup>17</sup> Heterozygous-null mice showed a reduced body weight and delayed motor development, and brain-specific conditional knock-out mice

demonstrated reduced spontaneous motor activity and grip strength of the hindlimbs.<sup>18</sup> Mice lacking cysteine-rich domain (CRD) isoforms of *Nrg-1* (*CRD-NRG-1*<sup>-/-</sup>) die perinatally as a result of respiratory failure, lack detectable limb movement, and exhibit a loss of ~60% of spinal motor neurons.<sup>19</sup> Similarly, motor and sensory neuron-specific conditional *Nrg-1* knockout mice die at birth and showed marked retraction of motor-neuron axons.<sup>20</sup> Furthermore, a decrease in the amount of CRD-NRG-1 has been detected in the spinal motor neurons in FALS and SALS individuals and *Sod1* mutant mice at disease onset,<sup>21</sup> raising the possibility that disruption of the NRG-ErbB pathway is commonly involved in the motor-neuron degeneration underlying ALS. This study provides insight into ALS pathogenesis and is expected to pave the way for the development of innovative therapeutic strategies such as using NRGs or their agonists to upregulate ErbB4 functions.

### Supplemental Data

Supplemental Data include two figures and four tables and can be found with this article online at <http://www.cell.com/AJHG/>.

### Consortia

Consortium members of JaCALS include Ryoichi Nakamura, Hazuki Watanabe, Yuishin Izumi, Ryuji Kaji, Mitsuya Morita, Kotaro Ogaki, Akira Taniguchi, Ikuko Aiba, Koichi Mizoguchi, Koichi Okamoto, Kazuko Hasegawa, Masashi Aoki, Akihiro Kawata, Imaharu Nakano, Koji Abe, Masaya Oda, Masaaki Konagaya, Takashi Imai, Masanori Nakagawa, Takuji Fujita, Hidenao Sasaki, and Masatoyo Nishizawa.

### Acknowledgments

We thank all the family members for participating in this study. This study was supported in part by KAKENHI (Grants-in-Aid for Scientific Research on Innovative Areas [22129001 and 22129002]) to S.T.; the Global COE Program from the Ministry of Education, Culture, Sports, Science, and Technology of Japan, and a grant-in-aid (H23-Jitsuyoka [Nanbyo]-Ippan-004) from the Ministry of Health, Labour, and Welfare, Japan to S.T. We acknowledge support to R.H.B. from ALS Therapy Alliance, Project ALS, P2ALS, the Angel Fund, the Pierre L. de Bourgnicht ALS Research Foundation, the Al-Athel ALS Research Foundation, the ALS Family Charitable Foundation, and grant 1R01NS050557 from the National Institute of Neurological Disorders and Stroke of the National Institutes of Health and support to G.A.N. from the MND Research Institute of Australia. P.G.-P. was supported by the Alfonso Martin Escudero Foundation (Madrid).

Received: May 12, 2013

Revised: August 26, 2013

Accepted: September 13, 2013

Published: October 10, 2013

### Web Resources

The URLs for data presented herein are as follows:

1000 Genomes Project Database, <http://www.1000genomes.org/>

dbSNP135, <http://www.ncbi.nlm.nih.gov/projects/SNP/>  
ExonPrimer, <http://ihg.gsf.de/ihg/ExonPrimer.html>  
NCBI37/hg19 assembly, <http://genome.ucsc.edu/>  
NHLBI GO Exome Sequencing Project (NHLBI-ESP), <https://esp.gs.washington.edu/drupal>  
Online Mendelian Inheritance in Man (OMIM), <http://www.omim.org/>  
Personal genome databases, <http://www.sequenceontology.org/resources/10Gen.html>  
PLINK algorithm, <http://pngu.mgh.harvard.edu/purcell/plink/>  
PolyPhen-2, <http://genetics.bwh.harvard.edu/pph2/>  
RefSeq, <http://www.ncbi.nlm.nih.gov/projects/RefSeq/>  
UCSC Human Genome Browser, <http://genome.ucsc.edu/>

### Accession Numbers

The dbSNP accession numbers for the c. 2780G>A and c. 3823C>T mutations reported for *ERBB4* in this paper are ss831884245 and ss831884246, respectively.

### References

1. Al-Chalabi, A., Jones, A., Troakes, C., King, A., Al-Sarraj, S., and van den Berg, L.H. (2012). The genetics and neuropathology of amyotrophic lateral sclerosis. *Acta Neuropathol.* *124*, 339–352.
2. Andersen, P.M., and Al-Chalabi, A. (2011). Clinical genetics of amyotrophic lateral sclerosis: what do we really know? *Nat Rev Neurol* *7*, 603–615.
3. Takahashi, Y., Seki, N., Ishiura, H., Mitsui, J., Matsukawa, T., Kishino, A., Onodera, O., Aoki, M., Shimozawa, N., Murayama, S., et al. (2008). Development of a high-throughput microarray-based resequencing system for neurological disorders and its application to molecular genetics of amyotrophic lateral sclerosis. *Arch. Neurol.* *65*, 1326–1332.
4. Ishiura, H., Takahashi, Y., Mitsui, J., Yoshida, S., Kihira, T., Kokubo, Y., Kuzuhara, S., Ranum, L.P., Tamaoki, T., Ichikawa, Y., et al. (2012). C9ORF72 repeat expansion in amyotrophic lateral sclerosis in the Kii peninsula of Japan. *Arch. Neurol.* *69*, 1154–1158.
5. Li, H., and Durbin, R. (2009). Fast and accurate short read alignment with Burrows-Wheeler transform. *Bioinformatics* *25*, 1754–1760.
6. Li, H., Handsaker, B., Wysoker, A., Fennell, T., Ruan, J., Homer, N., Marth, G., Abecasis, G., and Durbin, R.; 1000 Genome Project Data Processing Subgroup. (2009). The Sequence Alignment/Map format and SAMtools. *Bioinformatics* *25*, 2078–2079.
7. Robinson, J.T., Thorvaldsdóttir, H., Winckler, W., Guttman, M., Lander, E.S., Getz, G., and Mesirov, J.P. (2011). Integrative genomics viewer. *Nat. Biotechnol.* *29*, 24–26.
8. Fukuda, Y., Nakahara, Y., Date, H., Takahashi, Y., Goto, J., Miyashita, A., Kuwano, R., Adachi, H., Nakamura, E., and Tsuji, S. (2009). SNP HiTLink: a high-throughput linkage analysis system employing dense SNP data. *BMC Bioinformatics* *10*, 121.
9. Gudbjartsson, D.F., Thorvaldsdóttir, T., Kong, A., Gunnarsson, G., and Ingólfssdóttir, A. (2005). Allegro version 2. *Nat. Genet.* *37*, 1015–1016.
10. Purcell, S., Neale, B., Todd-Brown, K., Thomas, L., Ferreira, M.A., Bender, D., Maller, J., Sklar, P., de Bakker, P.I., Daly, M.J., and Sham, P.C. (2007). PLINK: a tool set for whole-genome association and population-based linkage analyses. *Am. J. Hum. Genet.* *81*, 559–575.

11. Kong, A., Frigge, M.L., Masson, G., Besenbacher, S., Sulem, P., Magnusson, G., Gudjonsson, S.A., Sigurdsson, A., Jonasdottir, A., Jonasdottir, A., et al. (2012). Rate of de novo mutations and the importance of father's age to disease risk. *Nature* *488*, 471–475.
12. Sanders, S.J., Murtha, M.T., Gupta, A.R., Murdoch, J.D., Raubeson, M.J., Willsey, A.J., Ercan-Sencicek, A.G., DiLullo, N.M., Parikshak, N.N., Stein, J.L., et al. (2012). De novo mutations revealed by whole-exome sequencing are strongly associated with autism. *Nature* *485*, 237–241.
13. Plowman, G.D., Green, J.M., Culouscou, J.M., Carlton, G.W., Rothwell, V.M., and Buckley, S. (1993). Heregulin induces tyrosine phosphorylation of HER4/p180erbB4. *Nature* *366*, 473–475.
14. Carpenter, G. (2003). ErbB-4: mechanism of action and biology. *Exp. Cell Res.* *284*, 66–77.
15. Sundvall, M., Korhonen, A., Vaparanta, K., Anckar, J., Halkilahti, K., Salah, Z., Aqeilan, R.I., Palvimo, J.J., Sistonen, L., and Elenius, K. (2012). Protein inhibitor of activated STAT3 (PIAS3) protein promotes SUMOylation and nuclear sequestration of the intracellular domain of ErbB4 protein. *J. Biol. Chem.* *287*, 23216–23226.
16. Pearson, R.J., Jr., and Carroll, S.L. (2004). ErbB transmembrane tyrosine kinase receptors are expressed by sensory and motor neurons projecting into sciatic nerve. *J. Histochem. Cytochem.* *52*, 1299–1311.
17. Gassmann, M., Casagrande, F., Orioli, D., Simon, H., Lai, C., Klein, R., and Lemke, G. (1995). Aberrant neural and cardiac development in mice lacking the ErbB4 neuregulin receptor. *Nature* *378*, 390–394.
18. Golub, M.S., Germann, S.L., and Lloyd, K.C.K. (2004). Behavioral characteristics of a nervous system-specific erbB4 knock-out mouse. *Behav. Brain Res.* *153*, 159–170.
19. Wolpowitz, D., Mason, T.B., Dietrich, P., Mendelsohn, M., Talmage, D.A., and Role, L.W. (2000). Cysteine-rich domain isoforms of the neuregulin-1 gene are required for maintenance of peripheral synapses. *Neuron* *25*, 79–91.
20. Yang, X., Arber, S., William, C., Li, L., Tanabe, Y., Jessell, T.M., Birchmeier, C., and Burden, S.J. (2001). Patterning of muscle acetylcholine receptor gene expression in the absence of motor innervation. *Neuron* *30*, 399–410.
21. Song, F., Chiang, P., Wang, J., Ravits, J., and Loeb, J.A. (2012). Aberrant neuregulin 1 signaling in amyotrophic lateral sclerosis. *J. Neuropathol. Exp. Neurol.* *71*, 104–115.

# Amyotrophic lateral sclerosis: an update on recent genetic insights

Yohei Iguchi · Masahisa Katsuno · Kensuke Ikenaka ·  
Shinsuke Ishigaki · Gen Sobue

Received: 31 August 2013/Revised: 10 September 2013/Accepted: 12 September 2013/Published online: 2 October 2013  
© Springer-Verlag Berlin Heidelberg 2013

**Abstract** Amyotrophic lateral sclerosis (ALS) is a devastating neurodegenerative disease affecting both upper and lower motor neurons. The prognosis for ALS is extremely poor, but there is a limited course of treatment with only one approved medication. A most striking recent discovery is that TDP-43 is identified as a key molecule that is associated with both sporadic and familial forms of ALS. TDP-43 is not only a pathological hallmark, but also a genetic cause for ALS. Subsequently, a number of ALS-causative genes have been found. Above all, the RNA-binding protein, such as FUS, TAF15, EWSR1 and hnRNPA1, have structural and functional similarities to TDP-43, and physiological functions of some molecules, including *VCP*, *UBQLN2*, *OPTN*, *FIG4* and *SQSTM1*, are involved in a protein degradation system. These discoveries provide valuable insight into the pathogenesis of ALS, and open doors for developing an effective disease-modifying therapy.

**Keywords** Amyotrophic lateral sclerosis · Motor neuron disease · Protein aggregation · RNA metabolism

## Introduction

Amyotrophic lateral sclerosis (ALS) is an adult-onset, progressive, and devastating neurodegenerative disease. The typical ALS case develops a muscle weakness and atrophy, which result from selective motor neuronal death in the cortex, brain stem, and spinal cord, but does not affect the oculomotor, sensory or autonomic functions. ALS occurs alone or with frontotemporal lobar degeneration (FTLD). Transactive response (TAR)-DNA binding protein 43 kDa (TDP-43) was identified as a component of the ubiquitinated neuronal inclusion in sporadic ALS (SALS) and FTLD with ubiquitinated inclusions [1–3]. These two diseases have been regarded as part of the spectrum of a single disease referred to as TDP-43 proteinopathy. TDP-43 is reported to be a causative molecule of familial ALS (FALS) [4–7]. Subsequently, a number of ALS-causative genes have been identified (<http://neuromuscular.wustl.edu/index.html>). Some of the identified ALS-causative molecules share physiological roles indispensable for a cellular activity and are involved in SALS pathologies (Fig. 1). Although the cause of SALS, which accounts for ~90 % of ALS, is uncertain, these discoveries have provided novel insights into the pathogenesis of ALS. Here we review recent genetic findings concerning ALS.

## TARDBP

In 2006, two groups reported that TDP-43 is a major component of ubiquitinated neuronal cytoplasmic inclusions in both SALS and FTLD [1, 2]. In addition, mutations of *TARDBP*, the gene encoding TDP-43, cause an autosomal dominant FALS, which accounts for ~5 % of FALS

Y. Iguchi · M. Katsuno · K. Ikenaka · S. Ishigaki ·  
G. Sobue (✉)  
Department of Neurology, Nagoya University Graduate School  
of Medicine, 65 Tsurumai-cho, Showa-ku, Nagoya 466-8550,  
Japan  
e-mail: sobueg@med.nagoya-u.ac.jp

Y. Iguchi  
The Centre de Recherche de l'Institut Universitaire en Santé  
Mentale de Québec-CRIUSMQ, Laval University,  
Québec, QC G1J 2G3, Canada

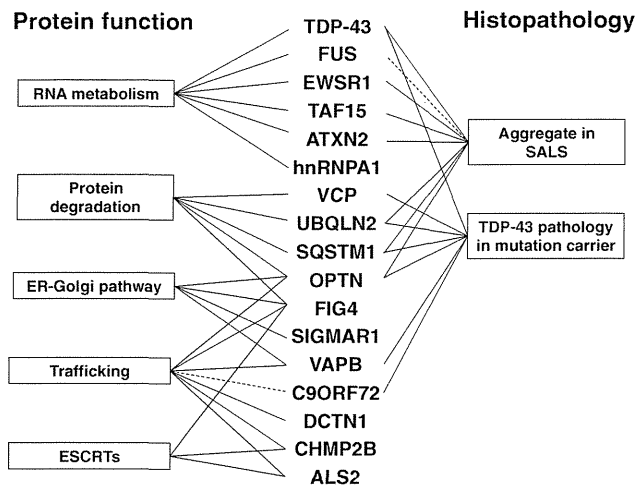


**Fig. 1** Physiological and neuropathological overlaps of ALS-causative genes. Several ALS-causing molecules share similar cellular functions and are possibly co-localized in intra-neuronal aggregates of ALS. Aggregate in SALS; the protein encoded by each gene forms aggregates in a SALS-affected region. TDP-43 pathology in mutation carrier; TDP-43-positive cytoplasmic inclusion is observed in ALS cases with each mutation. ESCRTs, endosomal sorting complexes required for transport

cases [4–7]. Except for D169G, all *TARDBP* mutations are in the C-terminal glycine-rich region encoded by exon 6. Although ALS patients carrying TDP-43 mutations normally exhibit a classical ALS phenotype with rare co-occurrence of dementia, there is a trend for disease onset to be earlier, with upper limb onset being more common and a longer duration compared to SALS patients [8]. TDP-43 is an RNA-binding protein that regulates elements of RNA metabolism such as gene transcription, stability of mRNA, pre-mRNA splicing, and microRNA biogenesis [9–18]. This protein is redistributed from the nucleus to the cytoplasm and forms aggregates in affected neurons and glial cells of SALS patients [1–3] (Fig. 2), suggesting that gain and/or loss of TDP-43 function underlies SALS pathogenesis. With regard to gain of TDP-43 toxicity, rodent and primate models overexpressing wild-type or disease-mutant

TDP-43 exhibit the phenotype of neurodegeneration, but this exogenous TDP-43 exists mainly in the nuclei, and TDP-43-positive cytoplasmic inclusions are barely detectable [19–28]. Although it is unclear how wild-type and mutant TDP-43 acquire a toxic effect, overexpression of TDP-43 makes a dose-dependent contribution to neurodegeneration [20–22]. In addition, pathological *TARDBP* mutations have longer half-lives compared to the wild type [29, 30], and longer half-lives of mutant proteins are correlated with accelerated disease onset [30], suggesting that mutant TDP-43 toxicity depends on its protein stability. On the other hand, *TARDBP* knockout mice are embryonic lethal [31–33], and postnatal deletion of *TARDBP* led to rapid loss of body fat and death [34]. Finally, motor neuron-specific *TARDBP* knockout mice exhibited age-dependent progressive motor dysfunction together with ALS-mimicking pathology, including motor axonal degeneration, neurogenic muscle atrophy, and denervation at neuromuscular junctions [35, 36] (Fig. 3). These lines of evidence suggest that both gain and loss of TDP-43 function contribute to ALS pathogenesis.

## FUS

Mutations in the gene encoding fused in sarcoma (*FUS*) mutations have been identified in autosomal dominant FALS, which accounts for ~4 % of FALS cases [37–39]. The majority of *FUS* mutations are in the C-terminal nuclear localization signal (NLS), and these mutants cause aberrant cytoplasmic distributions of *FUS* [37, 38]. Although the majority of patients carrying *FUS* mutations exhibit a classical ALS phenotype without cognitive impairment, the clinical courses of these ALS patients are diverse, even among carriers of the same mutations [40–44]. The *FUS* protein has been demonstrated in neuronal cytoplasmic inclusions in ALS cases with *FUS* mutations and a subset of FTLN with ubiquitinated, neuronal intermediate filament inclusion disease (NINID), and basophilic

**Fig. 2** TDP-43 pathology of spinal motor neuron. Lumbar spinal cords of control and ALS patients were stained with anti-TDP-43 antibody (Proteintech). TDP-43 is normally localized in the nucleus, but is redistributed to the cytoplasm in various patterns, such as a diffuse granular distribution (*arrow*) and skein-like inclusions (*arrow head*). The scale bars represent 20  $\mu$ m

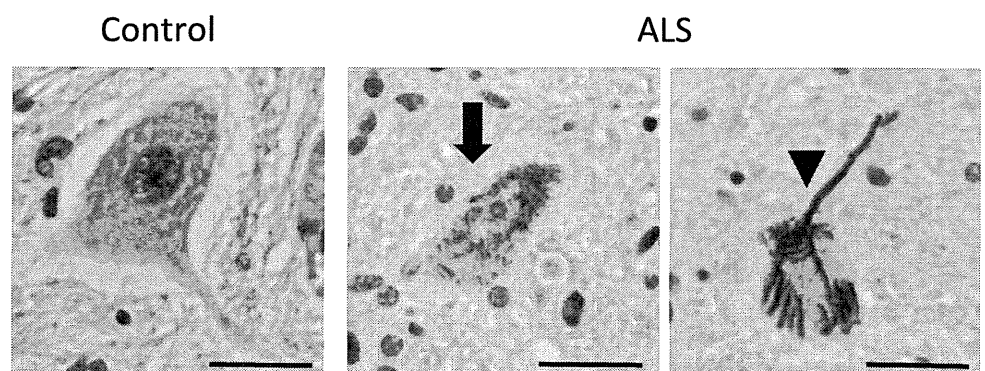
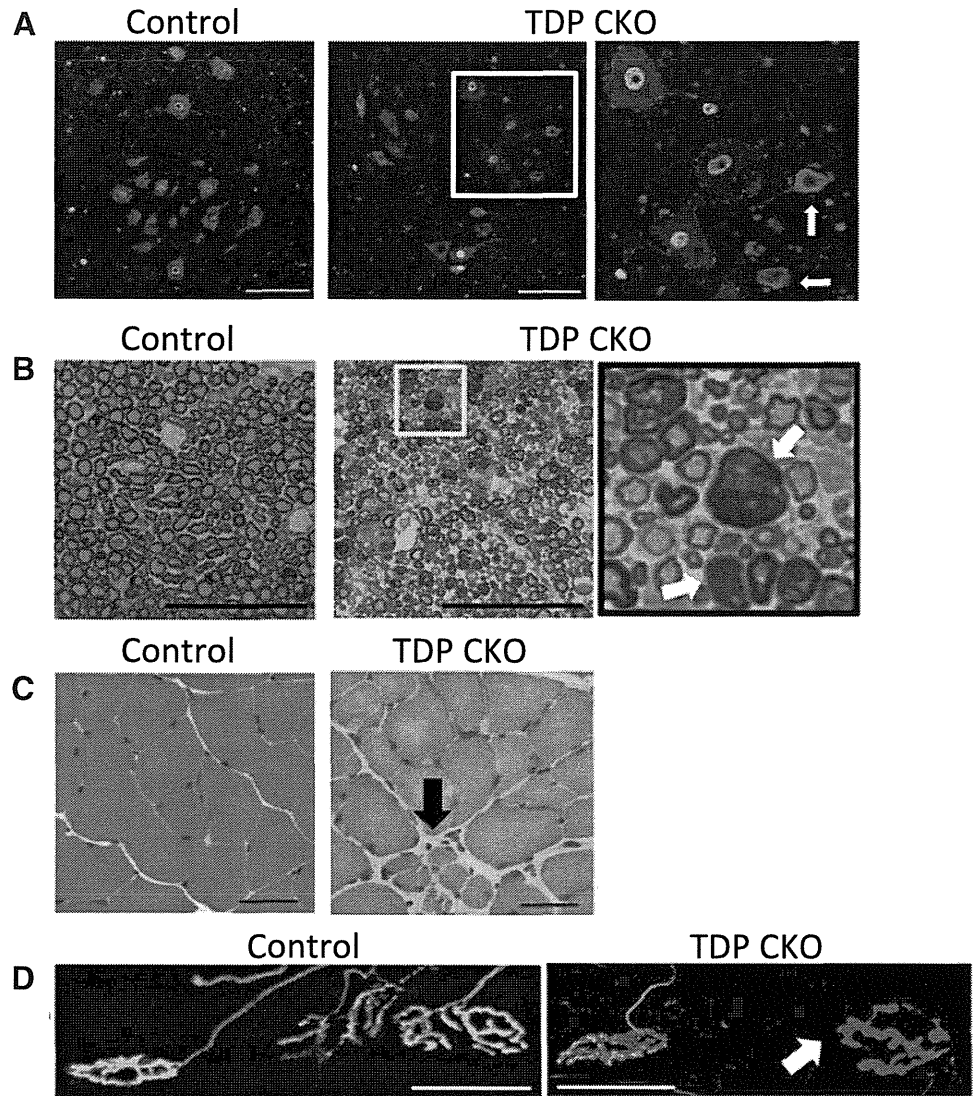


**Fig. 3** Motor neuron-specific TDP-43 knockout (TDP CKO) mice exhibit degeneration of the motor neuron system.  
**a** Immunofluorescent stainings (TDP-43, *green*; ChAT, *red*) of the lumbar ventral horn from 100-week-old control and TDP CKO mice. TDP-43-lacking motor neurons (*arrows*) were significantly smaller than TDP-43-positive motor neurons.  
**b** Toluidine blue-stained images in the L5 ventral root from 100-week-old control and TDP CKO mice. *Arrows* indicate axonal degeneration. The *scale bars* represent 100  $\mu$ m.  
**c** Hematoxylin and eosin staining of gastrocnemius muscles of 100-week-old mice. Axial sections from TDP CKO mice exhibited grouped atrophy (*arrow*).  
**d** Immunofluorescent staining (synaptophysin and phospho-neurofilament, *green*; bungarotoxin, *red*) of NMJs in 100-week-old mice. Denervated NMJs (*arrow*) are indicated by the lack of staining of synaptophysin and phospho-neurofilament. The *scale bar* represents 50  $\mu$ m. Reproduced with permission from Iguchi et al. Ref. [36]



inclusion body disease (BIBD) [45–48]. These inclusions are positive for GRP78/BiP, p62 and ubiquitin, but not for TDP-43 [38, 49, 50]. In addition, FUS is reported to be co-localized with ubiquitin and TDP-43-positive cytoplasmic inclusions of SALS patients [51, 52]. This issue remains controversial, however, because in other studies, FUS was not found in these inclusions in SALS [38, 47, 53]. Rat models overexpressing human disease mutants of *FUS* exhibit pathological phenotypes like ALS and FTL [54], and overexpression of human wild-type *FUS* in mice causes dose-dependent progressive motor neuron degeneration [55]. By contrast, *FUS* knockout mice on an inbred C57BL/6 background display perinatal death and exhibit abnormal lymphocytes and chromosomal instability [56], whereas knockout mice on an outbred background develop male sterility and survive until adulthood [57]. It is noteworthy that *FUS* and TDP-43 share structural and functional similarities [58] and that both proteins regulate alternative

pre-mRNA splicing events and transcription [59–62]. Although most of the mRNA targets for *FUS* are distinct from those for TDP-43, a small set of common targets may contribute to ALS pathogenesis [60, 61]. In addition, both TDP-43 and *FUS* associate with the SMN complex and are involved in spliceosome maintenance [63, 64].

**FIG4**

*FIG4* was reported as a causative gene for Charcot-Marie-Tooth disease type 4J (CMT4J), an autosomal recessive motor and sensory neuropathy [65]. Later, *FIG4* mutations were identified in autosomal-dominant FALS and SALS [66]. In this cohort of European ancestry, *FIG4* mutations were found in 2 % of ALS and primary lateral sclerosis (PLS) cases [66]. Two of ten identified mutations are truncation mutations that lead to loss of *FIG4* phosphatase

activity [66]. The protein transcript of *FIG4* is a phosphoinositide 5-phosphatase that regulates a cellular abundance of phosphatidylinositol 3,5-bisphosphate (PI(3,5)P<sub>2</sub>), a signaling lipid on the cytosolic surface of membranes of the late endosomal compartment [67]. PI(3,5)P<sub>2</sub> is required for retrograde membrane trafficking from lysosomal and late endosomal compartments to the Golgi and is involved in autophagy [68–70]. The analysis of *FIG4*<sup>-/-</sup> mouse brain shows disruption of autophagy in neurons and glial cells [71].

### OPTN

Three mutations of *OPTN* were identified in Japanese FALS patients [72], with both dominant and recessive mutations observed. Later analyses in Japanese and European populations revealed several additional mutations, and estimated mutation rates were 1–4 % in FALS [73–75]. Although optineurin, which is encoded by *OPTN*, regulates TNF $\alpha$ -induced NF- $\kappa$ B activation negatively by binding to polyubiquitinated RIP [76], ALS-causative *OPTN* mutations abolish its inhibition [72]. *OPTN* also acts as an autophagy receptor [77] and coordinates actin-based and microtubule-based motor function for maintenance of Golgi morphology [78]. *OPTN* is co-localized in ubiquitinated neuronal cytoplasmic inclusions of SALS spinal cords [72, 79–81], suggesting that *OPTN* is generally involved in the pathogenesis of a variety of ALS types.

### ATXN2

The pathological expansions (>34 repeats) of a CAG repeat in *ATXN2*, which encodes a polyglutamine tract in ataxin-2, cause spinocerebellar ataxia type 2 (SCA2). Intermediate-length expansions (27–33 glutamine residues) were reported to contribute to susceptibility to ALS [82]. In a later study, however, longer *ATXN2* repeats (>29–32 repeats) were significantly associated with the disease [83–86], and CAG repeats ( $\geq$ 32) were found in approximately 2 % of familial and sporadic ALS patients [84]. Furthermore, Expanded *ATXN2* repeats were also significantly associated with progressive supranuclear palsy [87]. Pathological analysis shows that ataxin-2 forms cytoplasmic aggregates in ALS spinal cord neurons, although this protein is localized in a diffuse or fine-granular pattern throughout the cytoplasm of control spinal cord neurons [82]. Although the pathological mechanism of *ATXN2* expansion in ALS pathogenesis is not fully understood, CAG repeat expansions are reported to enhance the interaction between ataxin-2 and TDP-43 or mutant FUS [82, 88].

### DAO

D-serine, a co-agonist of the *N*-methyl D-aspartate (NMDA) type of glutamate receptor [89], was reported to accumulate in the spinal cords of SALS and G93A SOD1 mice [90, 91]. D-amino acid oxidase (DAO) negatively regulates D-serine. Mutation R199W in the *DAO* gene was identified in autosomal dominant FALS [92]. This mutation, when expressed in neuronal cell lines, reduces cell viabilities and induces ubiquitinated aggregates [92]. These data suggest that accumulation of D-serine contributes to an ALS pathogenesis, and DAO might be a common therapeutic target for ALS.

### SPG11

Mutations of the spatacsin gene (*SPG11*) are the most common cause of hereditary spastic paraplegia with thinning corpus callosum [93]. Recently, *SPG11* mutations were identified in autosomal recessive juvenile ALS [94]. These patients exhibit a slowly progressive phenotype of motor neuron disease. Although the loss-of-function mechanism is suggested as the pathogenesis of ALS with the *SPG11* mutation, the physiological function of this molecule is unclear.

### VCP

Mutations in *VCP* were found in patients with inclusion body myopathy of early-onset Paget disease and frontotemporal dementia (IBMPFD) [95]. In addition, *VCP* mutation was identified in 1–2 % of FALS cases with or without the phenotype of IBMPFD in an autosomal dominant manner [96]. Now, IBMPFD is referred to as a multisystem proteinopathy (MSP), which affects motor neurons, brain, skeletal muscle, and bone. *VCP* mutation carriers exhibit diverse phenotypes, even with the same mutation [97]. TDP-43 positive ubiquitinated cytoplasmic inclusions in the affected neurons are present in patients with *VCP* mutations [96, 98]. The highly conserved AAA+-ATPase, *VCP* regulates multiple cellular pathways such as the ubiquitin–proteasome system (UPS), autophagy, endosomal sorting, and regulating protein degradation at the outer mitochondrial membrane, and chromatin-associated processes [99]. *VCP* is indispensable for maturation of autophagosomes, and disease-causative mutations of *VCP* disrupt this process [100]. Mutant *VCP* knock-in mice develop age-dependent motor dysfunction with abnormal TDP-43 pathologies in the spinal cord, muscle and brain [101–103].

## UBQLN2

Mutations in *UBQLN2* were identified in rare X-linked dominant ALS cases [104]. UBQLN2-positive inclusions are found in the spinal cord of ALS and ALS/FTLD patients with *UBQLN2* mutations, and these inclusions frequently contain TDP-43 and FUS [104, 105]. In addition, abnormal UBQLN2 pathologies are found in SALS patients and FUS mutation carriers [104, 105]. These data suggest that UBQLN2 is generally involved in the pathogenesis of ALS. UBQLN2 is a member of the ubiquilin family, which is involved in both the ubiquitin–proteasome system and autophagy [106, 107], and mutations in *UBQLN2* were reported to disrupt protein degradation [104].

## C9ORF72

In a large family with FTLD and/or ALS mapping to chromosome 9p21, a GGGGCC hexanucleotide repeat was identified between noncoding exons 1a and 1b of the *C9ORF72* gene [108, 109]. The repeat is <25 units in healthy controls, whereas the estimated expansion range is from 800 to 4,400 units in cases carrying this repeat expansion [108–110]. The mutation frequencies in European and North American Caucasian populations are generally high: they are up to 29, 50 and 88 % in FTLD, ALS and ALS/FTLD patients [111]. Especially in North Europe, the repeat expansion frequencies are from 12 to 21 %, even in the SALS patients [108, 112, 113]. By contrast, the frequency of ALS patients with these expansions is very low in Asian populations [113–119]. ALS patients with *C9ORF72* expansion commonly have a bulbar onset and cognitive impairment and partially exhibit Parkinsonism or psychiatric symptoms such as psychosis or suicide [120–122]. Abundant UBQLN-positive cytoplasmic inclusions are seen in the cerebellum and the hippocampus. UBQLN is co-localized partially with p62 and only rarely with TDP-43 positive inclusions [123, 124]. Using RNA fluorescence in situ hybridization (FISH) analysis, *C9ORF72*-containing RNA foci are observed in 25 % of the spinal cord and frontal cortical neurons of patients with the repeat expansion [108]. In addition, the neurons contain dipeptide repeat proteins generated from this intronic repeat region by non-ATG-initiated translation [125, 126]. It is, however, uncertain whether these neuronal accumulations of the aberrant RNA, and protein derived from *C9ORF72* repeat expansions contribute to the neurodegeneration. The latest study demonstrated that *C9ORF72* is a full-length distant homologue of proteins related to DENN, which is a Rab GEF, a regulator of Rab-GTPase activity [127]. Because Rab GTPases regulate membrane trafficking, *C9ORF72* may have a crucial role in neuronal activities such as

axonal transport and the autophagy-lysosome system. Although no reliable antibody for this protein is known, the intronic repeat expansions are reported to cause the loss of one or all alternatively spliced *C9ORF72* transcripts [108, 109, 128], suggesting that *C9ORF72* haploinsufficiency may underlie the pathogenesis of ALS patients carrying this repeat expansion. The high incidence of *C9ORF72* mutations in Caucasian ALS patients raises the possibility of the additional identification for ALS-causative gene mutations, even in SALS. Targeting a specific molecule, such as *C9ORF72*, appears to be a promising strategy.

## PFN1

*PFN1* mutations were identified in autosomal dominant FALS patients, [129]. Although four missense mutations were reported in 274 FALS patients [129], several other analyses further suggest that the mutation carriers in FALS patients are generally rare [130–138]. Profilin-1, the protein transcript of *PFN1*, is essential for the polymerization of monomeric G-actin to form filamentous actin [139]. A disrupted mutant of *PFN1* causes a growth cone arrest in embryonic motor neurons of *Drosophila* [140]. Although the neuropathology of an ALS patient with the *PFN1* mutation is not reported, ALS-related mutants of *PFN1* form ubiquitinated cytoplasmic aggregates when they are overexpressed in Neuro-2a cells or primary motor neurons [129]. In addition, the *PFN1* mutants reduce actin-binding ability, inhibit axonal outgrowth, and reduce the size of the growth cone in cultured cells or primary motor neurons [129]. These findings suggest that mutation-dependent disruption of *PFN1* function contributes to ALS pathogenesis via an alteration of the actin dynamic pathway.

## SIGMAR1

*SIGMAR1* is reported to be associated with juvenile amyotrophic sclerosis. A homozygous missense mutation, E102Q, in *SIGMAR1* gene was identified in autosomal recessive FALS from Saudi Arabia [141]. Patients carrying the *SIGMAR1* mutation exhibit the motor neuron disease phenotype at the age of 1–2 years, and the weakness progresses slowly without cognitive impairment. The sigma-1 receptor (S1R), which is encoded by *SIGMAR1*, is a non-steroidal ER protein that regulates various ion channel activities and has a protein chaperone function [142]. S1R is highly expressed in motor neurons of the brain stem and spinal cord, and S1R knockout mice are reported to have motor deficiency [143]. These findings suggest that the mutation in *SIGMAR1* affects predominantly motor neurons via loss of S1R function. Further investigations,

including a histopathological characterization of post-mortem samples and functional analysis of the S1R mutant, are needed.

### Molecular targeted approach for the treatment of ALS

Current therapies for neurodegenerative diseases are targeted mainly to symptomatic relief or replacement of neurotransmitters. Most of these therapies, however, do not halt or reduce neurodegenerative progression [144]. With regard to ALS, the only available drug, riluzole (6-(trifluoromethoxy)benzothiazol-2-amine), has a limited effect: the increase in median survival for the riluzole-treated group was 2–3 months [145]. Many compounds, including vitamin E, gabapentin, topiramate, creatine, celecoxib and minocycline, identified in studies using animal models have failed in the clinical trials of ALS.

Although several interpretations can be considered, one possibility of the cause of this divergence is the use of mutant SOD1 mice in pre-clinical studies. There are distinct pathophysiological differences between SOD1-mediated FALS (ALS1) and SALS [146, 147]. Conversely, TDP-43 is a promising therapeutic target for SALS, because abnormal TDP-43 pathologies are characteristic features of SALS. Given that a dose-dependent or aggregate toxicity of TDP-43 would be related to ALS pathogenesis, interventions to regulate TDP-43 protein expression or to mitigate the aggregate formation could have therapeutic potential for ALS. An analysis using induced pluripotent stem (iPS) cells derived from ALS patients carrying TDP-43 mutations would be a useful tool for elucidating ALS disease pathogenesis and for screening drug candidates [148].

Analyzing functional similarities to ALS-causative molecules is a promising approach. Some of these molecules share physiological functions indispensable for cellular activities, including RNA metabolism, protein degradation, and the ER-Golgi pathway (Fig. 1). For instance, several ALS-causative genes, including *VCP*, *UBQLN2*, *OPTN* and *FIG4*, are related to a protein-degrading system via autophagy, and mutations in *SQSTM1*, which encodes p62, have been identified in ALS patients [149]. ALS patients carrying mutations in these genes have TDP-43-positive neuronal cytoplasmic inclusions, suggesting that the effect of these mutations could be an upstream cause for the aberrant TDP-43 pathology. In addition, p62-positive neuronal inclusions are seen in most of SALS and FALS patients, and accumulations of autophagosomes are observed in the motor neurons of SALS patients [150]. These lines of data suggest that dysregulation of autophagy commonly underlies ALS pathogenesis. Notably, autophagy activators rescue the phenotype and pathology in FTL model mice in which wild-type TDP-43 was overexpressed in the forebrain [151], suggesting

that the autophagic pathway could be a potential therapeutic target for ALS.

TDP-43, FUS, and ataxin-2 are components of stress granules (SGs), which have a central role in the stress response, such as regulating mRNA translation and turnover [152] under stress [153–155]. In addition, the TDP-43 C-terminal fragment and FUS-disease mutant are recruited more abundantly into SGs [156–158]. Given that stress granule marker proteins are co-localized in TDP-43 and FUS-positive neuronal inclusions of ALS and FTL patients [158, 159], dysregulation of mRNA metabolism in SGs would underlie common ALS pathogenesis and could be a therapeutic target for ALS. Furthermore, TDP-43 and FUS have a similar sequence to the prion protein, prion-like domain (PrLD). Notably, an insoluble fraction of TDP-43 from FTL brain has a seeding ability when introduced into cultured cells, and the aggregated TDP-43 induced by these seeds is propagated to neighboring cells [160]. These data suggest that interference with the propagation of TDP-43 or other RNA-binding proteins may be a therapeutic target for ALS. Finally, mutations in other RNA-binding proteins, such as Ewing's sarcoma breakpoint region 1 (EWSR1), TATA-binding protein-associated factor 15 (TAF15), and heterogeneous nuclear ribonucleoprotein A1 (hnRNPA1) have been identified in ALS patients [161–163]. These RNA-binding proteins are responsible for RNA metabolism and harbor a PrLD as well as TDP-43 and FUS.

ALS causative genes have been uncovered by recent developments in gene analysis technology. Certain FALS-causing gene mutations have also been identified in SALS cases, suggesting that sporadic and familial forms of ALS share, at least in part, the same molecular pathomechanism. These discoveries provide novel insight into ALS pathogenesis and are expected to contribute to developing an effective disease-modifying therapy. Given the limited availability of animal models carrying FALS mutations, the results of genetic studies should be utilized for the creation of models and the search for therapies that suppress motor neuron degeneration.

**Acknowledgments** This work was supported by Grant-in-Aids (KAKENHI) from the Ministry of Education, Culture, Sports, Science, and Technology of Japan (Nos. 22110005, 21229011 and 23390230) and Core Research for Evolutional Science and Technology (CREST) from the Japan Science and Technology Agency (JST). Figure 3 was reproduced from Iguchi et al. Ref. [36].

**Conflicts of interest** None.

### References

1. Arai T, Hasegawa M, Akiyama H et al (2006) TDP-43 is a component of ubiquitin-positive tau-negative inclusions in

- frontotemporal lobar degeneration and amyotrophic lateral sclerosis. *Biochem Biophys Res Commun* 351:602–611
2. Neumann M, Sampathu DM, Kwong LK et al (2006) Ubiquitinated TDP-43 in frontotemporal lobar degeneration and amyotrophic lateral sclerosis. *Science* 314:130–133
  3. Mackenzie IR, Neumann M, Cairns NJ et al (2011) Novel types of frontotemporal lobar degeneration: beyond tau and TDP-43. *J Mol Neurosci* 45:402–408
  4. Gitcho MA, Baloh RH, Chakraverty S et al (2008) TDP-43 A315T mutation in familial motor neuron disease. *Ann Neurol* 63:535–538
  5. Kabashi E, Valdmanis PN, Dion P et al (2008) TARDBP mutations in individuals with sporadic and familial amyotrophic lateral sclerosis. *Nat Genet* 40:572–574
  6. Sreedharan J, Blair IP, Tripathi VB et al (2008) TDP-43 mutations in familial and sporadic amyotrophic lateral sclerosis. *Science* 319:1668–1672
  7. Yokoseki A, Shiga A, Tan CF et al (2008) TDP-43 mutation in familial amyotrophic lateral sclerosis. *Ann Neurol* 63:538–542
  8. Corcia P, Valdmanis P, Millicamps S et al (2012) Phenotype and genotype analysis in amyotrophic lateral sclerosis with TARDBP gene mutations. *Neurology* 78:1519–1526
  9. Wang HY, Wang IF, Bose J et al (2004) Structural diversity and functional implications of the eukaryotic TDP gene family. *Genomics* 83:130–139
  10. Ayala YM, Pantano S, D'Ambrogio A et al (2005) Human, *Drosophila*, and *C. elegans* TDP43: nucleic acid binding properties and splicing regulatory function. *J Mol Biol* 348:575–588
  11. Buratti E, Brindisi A, Giombi M et al (2005) TDP-43 binds heterogeneous nuclear ribonucleoprotein A/B through its C-terminal tail: an important region for the inhibition of cystic fibrosis transmembrane conductance regulator exon 9 splicing. *J Biol Chem* 280:37572–37584
  12. Strong MJ, Volkening K, Hammond R et al (2007) TDP43 is a human low molecular weight neurofilament (hNFL) mRNA-binding protein. *Mol Cell Neurosci* 35:320–327
  13. Buratti E, De Conti L, Stuardi C et al (2010) Nuclear factor TDP-43 can affect selected microRNA levels. *FEBS J* 277:2268–2281
  14. Polymenidou M, Lagier-Tourenne C, Hutt KR et al (2011) Long pre-mRNA depletion and RNA missplicing contribute to neuronal vulnerability from loss of TDP-43. *Nat Neurosci* 14:459–468
  15. Tollervy JR, Curk T, Rogelj B et al (2011) Characterizing the RNA targets and position-dependent splicing regulation by TDP-43. *Nat Neurosci* 14:452–458
  16. Sephton CF, Cenik C, Kucukural A et al (2011) Identification of neuronal RNA targets of TDP-43-containing ribonucleoprotein complexes. *J Biol Chem* 286:1204–1215
  17. Xiao S, Sanelli T, Dib S et al (2011) RNA targets of TDP-43 identified by UV-CLIP are deregulated in ALS. *Mol Cell Neurosci* 47:167–180
  18. Kawahara Y, Mieda-Sato A (2012) TDP-43 promotes microRNA biogenesis as a component of the Drosha and Dicer complexes. *Proc Natl Acad Sci USA* 109:3347–3352
  19. Wegorzewska I, Bell S, Cairns NJ et al (2009) TDP-43 mutant transgenic mice develop features of ALS and frontotemporal lobar degeneration. *Proc Natl Acad Sci USA* 106:18809–18814
  20. Wils H, Kleinberger G, Janssens J et al (2010) TDP-43 transgenic mice develop spastic paralysis and neuronal inclusions characteristic of ALS and frontotemporal lobar degeneration. *Proc Natl Acad Sci USA* 107:3858–3863
  21. Xu YF, Gendron TF, Zhang YJ et al (2010) Wild-type human TDP-43 expression causes TDP-43 phosphorylation, mitochondrial aggregation, motor deficits, and early mortality in transgenic mice. *J Neurosci* 30:10851–10859
  22. Stallings NR, Puttapparthi K, Luther CM et al (2010) Progressive motor weakness in transgenic mice expressing human TDP-43. *Neurobiol Dis* 40:404–414
  23. Zhou H, Huang C, Chen H et al (2010) Transgenic rat model of neurodegeneration caused by mutation in the TDP gene. *PLoS Genet* 6:e1000887
  24. Tsai KJ, Yang CH, Fang YH et al (2010) Elevated expression of TDP-43 in the forebrain of mice is sufficient to cause neurological and pathological phenotypes mimicking FTLD-U. *J Exp Med* 207:1661–1673
  25. Shan X, Chiang PM, Price DL et al (2010) Altered distributions of Gemini of coiled bodies and mitochondria in motor neurons of TDP-43 transgenic mice. *Proc Natl Acad Sci USA* 107:16325–16330
  26. Swarup V, Phaneuf D, Bareil C et al (2011) Pathological hallmarks of amyotrophic lateral sclerosis/frontotemporal lobar degeneration in transgenic mice produced with TDP-43 genomic fragments. *Brain* 134:2610–2626
  27. Arnold ES, Ling SC, Huelga SC et al (2013) ALS-linked TDP-43 mutations produce aberrant RNA splicing and adult-onset motor neuron disease without aggregation or loss of nuclear TDP-43. *Proc Natl Acad Sci USA* 110:E736–E745
  28. Uchida A, Sasaguri H, Kimura N et al (2012) Non-human primate model of amyotrophic lateral sclerosis with cytoplasmic mislocalization of TDP-43. *Brain* 135:833–846
  29. Ling SC, Albuquerque CP, Han JS et al (2010) ALS-associated mutations in TDP-43 increase its stability and promote TDP-43 complexes with FUS/TLS. *Proc Natl Acad Sci USA* 107:13318–13323
  30. Watanabe S, Kaneko K, Yamanaka K (2013) Accelerated disease onset with stabilized familial amyotrophic lateral sclerosis (ALS)-linked mutant TDP-43 proteins. *J Biol Chem* 288:3641–3654
  31. Wu LS, Cheng WC, Hou SC et al (2010) TDP-43, a neuro-pathosignature factor, is essential for early mouse embryogenesis. *Genesis* 48:56–62
  32. Sephton CF, Good SK, Atkin S et al (2010) TDP-43 is a developmentally regulated protein essential for early embryonic development. *J Biol Chem* 285:6826–6834
  33. Kraemer BC, Schuck T, Wheeler JM et al (2010) Loss of murine TDP-43 disrupts motor function and plays an essential role in embryogenesis. *Acta Neuropathol* 119:409–419
  34. Chiang PM, Ling J, Jeong YH et al (2010) Deletion of TDP-43 down-regulates *Tbc1d1*, a gene linked to obesity, and alters body fat metabolism. *Proc Natl Acad Sci USA* 107:16320–16324
  35. Wu LS, Cheng WC, Shen CK (2012) Targeted depletion of TDP-43 expression in the spinal cord motor neurons leads to the development of amyotrophic lateral sclerosis-like phenotypes in mice. *J Biol Chem* 287:27335–27344
  36. Iguchi Y, Katsuno M, Niwa J et al (2013) Loss of TDP-43 causes age-dependent progressive motor neuron degeneration. *Brain* 136:1371–1382
  37. Kwiatkowski TJ Jr, Bosco DA, Leclerc AL et al (2009) Mutations in the FUS/TLS gene on chromosome 16 cause familial amyotrophic lateral sclerosis. *Science* 323:1205–1208
  38. Vance C, Rogelj B, Hortobagyi T et al (2009) Mutations in FUS, an RNA processing protein, cause familial amyotrophic lateral sclerosis type 6. *Science* 323:1208–1211
  39. Van Langenhove T, van der Zee J, Sleegers K et al (2010) Genetic contribution of FUS to frontotemporal lobar degeneration. *Neurology* 74:366–371
  40. Yan J, Deng HX, Siddique N et al (2010) Frameshift and novel mutations in FUS in familial amyotrophic lateral sclerosis and ALS/dementia. *Neurology* 75:807–814

41. Mackenzie IR, Ansorge O, Strong M et al (2011) Pathological heterogeneity in amyotrophic lateral sclerosis with FUS mutations: two distinct patterns correlating with disease severity and mutation. *Acta Neuropathol* 122:87–98
42. Groen EJ, van Es MA, van Vught PW et al (2010) FUS mutations in familial amyotrophic lateral sclerosis in the Netherlands. *Arch Neurol* 67:224–230
43. Hara M, Minami M, Kamei S et al (2012) Lower motor neuron disease caused by a novel FUS/TLS gene frameshift mutation. *J Neurol* 259:2237–2239
44. Yamashita S, Mori A, Sakaguchi H et al (2012) Sporadic juvenile amyotrophic lateral sclerosis caused by mutant FUS/TLS: possible association of mental retardation with this mutation. *J Neurol* 259:1039–1044
45. Munoz DG, Neumann M, Kusaka H et al (2009) FUS pathology in basophilic inclusion body disease. *Acta Neuropathol* 118:617–627
46. Neumann M, Rademakers R, Roeber S et al (2009) A new subtype of frontotemporal lobar degeneration with FUS pathology. *Brain* 132:2922–2931
47. Neumann M, Roeber S, Kretzschmar HA et al (2009) Abundant FUS-immunoreactive pathology in neuronal intermediate filament inclusion disease. *Acta Neuropathol* 118:605–616
48. Seelaar H, Klijnsma KY, de Koning I et al (2010) Frequency of ubiquitin and FUS-positive, TDP-43-negative frontotemporal lobar degeneration. *J Neurol* 257:747–753
49. Tateishi T, Hokonohara T, Yamasaki R et al (2010) Multiple system degeneration with basophilic inclusions in Japanese ALS patients with FUS mutation. *Acta Neuropathol* 119:355–364
50. Suzuki N, Aoki M, Warita H et al (2010) FALS with FUS mutation in Japan, with early onset, rapid progress and basophilic inclusion. *J Hum Genet* 55:252–254
51. Deng HX, Zhai H, Bigio EH et al (2010) FUS-immunoreactive inclusions are a common feature in sporadic and non-SOD1 familial amyotrophic lateral sclerosis. *Ann Neurol* 67:739–748
52. Keller BA, Volkering K, Droppelmann CA et al (2012) Co-aggregation of RNA binding proteins in ALS spinal motor neurons: evidence of a common pathogenic mechanism. *Acta Neuropathol* 124:733–747
53. Huang EJ, Zhang J, Geser F et al (2010) Extensive FUS-immunoreactive pathology in juvenile amyotrophic lateral sclerosis with basophilic inclusions. *Brain Pathol* 20:1069–1076
54. Huang C, Zhou H, Tong J et al (2011) FUS transgenic rats develop the phenotypes of amyotrophic lateral sclerosis and frontotemporal lobar degeneration. *PLoS Genet* 7:e1002011
55. Mitchell JC, McGoldrick P, Vance C et al (2013) Overexpression of human wild-type FUS causes progressive motor neuron degeneration in an age- and dose-dependent fashion. *Acta Neuropathol* 125:273–288
56. Hicks GG, Singh N, Nashabi A et al (2000) FUS deficiency in mice results in defective B-lymphocyte development and activation, high levels of chromosomal instability, and perinatal death. *Nat Genet* 24:175–179
57. Kuroda M, Sok J, Webb L et al (2000) Male sterility and enhanced radiation sensitivity in TLS (–/–) mice. *EMBO J* 19:453–462
58. Lagier-Tourenne C, Cleveland DW (2009) Rethinking ALS: the FUS about TDP-43. *Cell* 136:1001–1004
59. Ishigaki S, Masuda A, Fujioka Y et al (2012) Position-dependent FUS-RNA interactions regulate alternative splicing events and transcriptions. *Sci Rep* 2:529
60. Lagier-Tourenne C, Polymenidou M, Hutt KR et al (2012) Divergent roles of ALS-linked proteins FUS/TLS and TDP-43 intersect in processing long pre-mRNAs. *Nat Neurosci* 15:1488–1497
61. Rogelj B, Easton LE, Bogu GK et al (2012) Widespread binding of FUS along nascent RNA regulates alternative splicing in the brain. *Sci Rep* 2:603
62. Nakaya T, Alexiou P, Maragkakis M et al (2013) FUS regulates genes coding for RNA-binding proteins in neurons by binding to their highly conserved introns. *RNA* 19:498–509
63. Tsujii H, Iguchi Y, Furuya A et al (2013) Spliceosome integrity is defective in the motor neuron diseases ALS and SMA. *EMBO Mol Med* 5:221–234
64. Yamazaki T, Chen S, Yu Y et al (2012) FUS-SMN protein interactions link the motor neuron diseases ALS and SMA. *Cell Rep* 2:799–806
65. Chow CY, Zhang Y, Dowling JJ et al (2007) Mutation of FIG4 causes neurodegeneration in the pale tremor mouse and patients with CMT4 J. *Nature* 448:68–72
66. Chow CY, Landers JE, Bergren SK et al (2009) Deleterious variants of FIG4, a phosphoinositide phosphatase, in patients with ALS. *Am J Hum Genet* 84:85–88
67. Volpicelli-Daley L, De Camilli P (2007) Phosphoinositides' link to neurodegeneration. *Nat Med* 13:784–786
68. Rutherford AC, Traer C, Wassmer T et al (2006) The mammalian phosphatidylinositol 3-phosphate 5-kinase (PIKfyve) regulates endosome-to-TGN retrograde transport. *J Cell Sci* 119:3944–3957
69. Zhang Y, Zolov SN, Chow CY et al (2007) Loss of Vac14, a regulator of the signaling lipid phosphatidylinositol 3,5-bisphosphate, results in neurodegeneration in mice. *Proc Natl Acad Sci USA* 104:17518–17523
70. Ferguson CJ, Lenk GM, Meisler MH (2010) PtdIns(3,5)P2 and autophagy in mouse models of neurodegeneration. *Autophagy* 6:170–171
71. Ferguson CJ, Lenk GM, Meisler MH (2009) Defective autophagy in neurons and astrocytes from mice deficient in PI(3,5)P2. *Hum Mol Genet* 18:4868–4878
72. Maruyama H, Morino H, Ito H et al (2010) Mutations of optineurin in amyotrophic lateral sclerosis. *Nature* 465:223–226
73. Del Bo R, Tiloca C, Pensato V et al (2011) Novel optineurin mutations in patients with familial and sporadic amyotrophic lateral sclerosis. *J Neurol Neurosurg Psychiatry* 82:1239–1243
74. Millicamps S, Boillee S, Chabrol E et al (2011) Screening of OPTN in French familial amyotrophic lateral sclerosis. *Neurobiol Aging* 32(557):e511–e553
75. Iida A, Hosono N, Sano M et al (2012) Optineurin mutations in Japanese amyotrophic lateral sclerosis. *J Neurol Neurosurg Psychiatry* 83:233–235
76. Zhu G, Wu CJ, Zhao Y et al (2007) Optineurin negatively regulates TNF $\alpha$ -induced NF- $\kappa$ B activation by competing with NEMO for ubiquitinated RIP. *Curr Biol* 17:1438–1443
77. Wild P, Farhan H, McEwan DG et al (2011) Phosphorylation of the autophagy receptor optineurin restricts Salmonella growth. *Science* 333:228–233
78. Sahlender DA, Roberts RC, Arden SD et al (2005) Optineurin links myosin VI to the Golgi complex and is involved in Golgi organization and exocytosis. *J Cell Biol* 169:285–295
79. Deng HX, Bigio EH, Zhai H et al (2011) Differential involvement of optineurin in amyotrophic lateral sclerosis with or without SOD1 mutations. *Arch Neurol* 68:1057–1061
80. Hortobagyi T, Troakes C, Nishimura AL et al (2011) Optineurin inclusions occur in a minority of TDP-43 positive ALS and FTLTDP cases and are rarely observed in other neurodegenerative disorders. *Acta Neuropathol* 121:519–527
81. Osawa T, Mizuno Y, Fujita Y et al (2011) Optineurin in neurodegenerative diseases. *Neuropathology* 31:569–574
82. Elden AC, Kim HJ, Hart MP et al (2010) Ataxin-2 intermediate-length polyglutamine expansions are associated with increased risk for ALS. *Nature* 466:1069–1075